Current Biology

Ancient and modern stickleback genomes reveal the demographic constraints on adaptation

--Manuscript Draft--

Manuscript Number:	CURRENT-BIOLOGY-D-20-02016R2
Full Title:	Ancient and modern stickleback genomes reveal the demographic constraints on adaptation
Article Type:	Report
Corresponding Author:	Andrew Foote University of Copenhagen Copenhagen, DENMARK
First Author:	Andrew Foote
Order of Authors:	Andrew Foote
	Anders Romundset
	Tom Gilbert
	Melanie Kirch
	Felicity Jones
Abstract:	Adaptation is typically studied by comparing modern populations from contrasting environments. Individuals persisting in the ancestral habitat are typically used to represent the ancestral founding population, however, it has been questioned whether these individuals are good proxies for the actual ancestors 1 . To address this, we applied a paleogenomics approach 2 to directly access the ancestral genepool: partially sequencing the genomes of two 11-13,000-year-old stickleback recovered from the transitionary layer between marine and freshwater sediments of two Norwegian isolation lakes 3 , and comparing them with 30 modern stickleback genomes from the same lakes and adjacent marine fjord, in addition to a global dataset of 20 genomes 4 . The ancient stickleback shared genome-wide ancestry with the modern fjord population, whereas modern lake populations have lost substantial ancestral variation following founder effects, and subsequent drift and selection. Freshwater-adaptive alleles found in one ancient stickleback genome have not risen to high frequency in the present-day population from the same lake. Comparison to the global dataset suggested incomplete adaptation to freshwater in our modern lake populations. Our findings reveal the impact of population bottlenecks in constraining adaptation due to reduced efficacy of selection on standing variation present in founder populations.

Ancient and modern stickleback genomes reveal the demographic constraints on adaptation

Melanie Kirch[1], Anders Romundset[2], M. Thomas P. Gilbert[3,4], Felicity C. Jones[1≪], Andrew D. Foote[4,5*≪]

[1]Friedrich Miescher Laboratory of the Max Planck Society, Max-Planck-Ring 9, 72076 Tübingen, Germany
[2]Geological Survey of Norway, Trondheim, Norway
[3]Center for Evolutionary Hologenomics, The GLOBE Institute, University of Copenhagen, Øster Farimagsgade 5A, DK-1353 Copenhagen, Denmark
[4]Department of Natural History, Norwegian University of Science and Technology (NTNU), University Museum, 7491 Trondheim, Norway
[5]Molecular Ecology and Fisheries Genetics Laboratory, School of Biological Sciences, Bangor University, Bangor, UK

≪Co-senior authors
*Correspondence and Lead Contact: Andrew.Foote@ntnu.no

SUMMARY

Adaptation is typically studied by comparing modern populations from contrasting environments. Individuals persisting in the ancestral habitat are typically used to represent the ancestral founding population, however, it has been questioned whether these individuals are good proxies for the actual ancestors [1]. To address this, we applied a paleogenomics approach [2] to directly access the ancestral genepool: partially sequencing the genomes of two 11-13,000-year-old stickleback recovered from the transitionary layer between marine and freshwater sediments of two Norwegian isolation lakes [3], and comparing them with 30 modern stickleback genomes from the same lakes and adjacent marine fjord, in addition to a global dataset of 20 genomes [4]. The ancient stickleback shared genome-wide ancestry with the modern fjord population, whereas modern lake populations have lost substantial ancestral variation following founder effects, and subsequent drift and selection. Freshwater-adaptive alleles found in one ancient stickleback genome have not risen to high frequency in the present-day population from the same lake. Comparison to the global dataset suggested incomplete adaptation to freshwater in our modern lake populations. Our findings reveal the impact of population bottlenecks in constraining adaptation due to reduced efficacy of selection on standing variation present in founder populations.

RESULTS AND DISCUSSION

The threespine stickleback *Gasterosteus aculeatus* genome is well characterised through mapping, sequencing and transgenics studies, which have provided a strong basis for understanding the role of genes underlying phenotypic changes in skeletal armour, body shape and other morphological and physiological changes associated with freshwater or marine adaptation [5,6]. Adaptation of marine sticklebacks to freshwater habitats can occur rapidly over tens of generations [7,8], facilitated by the reuse of pre-existing genetic variation carried in ancient haplotype blocks within the marine population [4,9,10]. This standing genetic variation is thought to have been maintained over geological timescales [9,11] through recurrent migration between freshwater and marine populations [12], and thus repeatedly acted upon by natural selection in freshwater populations [4,13]. The present adaptive radiation commenced during the transition between the Pleistocene and Holocene epochs, and from glacial to inter-glacial [5]. Investigating signatures of freshwater adaptation in the genomes of stickleback from this key time point in their evolutionary history has not been possible until now.

Here, we demonstrate the power of paleogenomics to provide novel temporal insights into evolutionary processes by sequencing partial genomes of two 11-13,000-year-old stickleback, which lived during the period immediately after the latest retreat of the Pleistocene Scandinavian Ice Sheet, when many freshwater coastal lakes were forming due to strong post-glacial land uplift. 'Isolation basins' formed by glacio-isostatic rebound, elevating them above sea-level, and rapidly changed from marine to freshwater ecosystems [14]. This ecological change causes a distinct sedimentary boundary between the marine and freshwater lacustrine sediment facies (Figures 1B, and S1) and is used by geologists to reconstruct relative sea-level history [14]. We examined sediment cores collected from freshwater lakes formed from isolation basins in Finnmark, northernmost Norway (Figures 1A, and S1), an area where post-glacial uplift has caused a net relative sea-level fall of 50-100 m since deglaciation [3].

Stickleback bones, spines and bony armour plates were found in the layers of cores from two lakes corresponding to the brackish phase when the lakes became isolated from the marine fjord and were transitioning to freshwater (Figures 1C, and S1). Radiocarbon dating of organic matter from the same stratigraphic depth placed the age of the stickleback bones as 12,040-11,410 cal yr BP for Lake 1 and 13,070–12,800 cal yr BP for Lake 2 (Figure 1B). Shotgun sequencing was performed on DNA extracted from a stickleback spine from Lake 1, and a bony armour plate

from Lake 2 (Figures 1C, and S1) resulting in coverage of ≥1× at 369,344 bp and 16,923,179 bp respectively. Nucleotide misincorporations relative to the reference genome indicate an approximately 30% deamination rate of cytosine at the read-ends (Methods S1 section 1). Such post-mortem damage patterns are characteristic of degradation in ancient DNA samples that are thousands of years old [15], and do not represent contamination from exogenous modern DNA. To the best of our knowledge, these are the oldest fish bones from which genomic data have been obtained [16]. Whilst these data represent just a single ancestor from each lake, their genomes potentially contain ancestry from >1,000 individuals from the previous ten generations (equivalent to 10-20 years). Single samples have routinely been used as representative examples of ancestral populations in palaeogenomics [17,18,19] and even partial genomes have provided key and novel insights into our understanding of evolutionary histories [20].

To understand the importance of the ancient samples in the chronology of freshwater adaptation, we first established their relationships to present-day sticklebacks. Uneven sampling of different demes can influence the inference of population clusters in Principal Component Analysis (PCA), due to strong covariance in allele frequencies among samples from the same population [21]. We therefore included a single randomly sampled haploid genome, removing coverage bias, from each of 23 present-day populations from geographically distant locations across the Northern Hemisphere [4] (hereafter referred to as the 'global' population dataset Table S1), and considered only transversions to avoid post-mortem DNA damage patterns of excess C→T and A→G changes resulting from deamination [15]. Samples separate by geography into Pacific and Atlantic clusters on principal component 1 (PC1, $P < 0.001$; Figures 2A; Methods S1 section 2) when genomic regions underlying parallel marine-freshwater adaptive divergence [4] are excluded. Both ancient samples show closest affinity to present-day Atlantic populations, as expected. An analysis using only marine-freshwater parallel divergent genomic regions, separates samples into marine and freshwater ecotypes on PC1 and revealed both ancient samples cluster with the globally sampled marine individuals ($P < 0.005$; Figures 2A; Methods S1 section 2). Under a polygenic model this suggests that the two ancient fish would have had a predominantly marine phenotype.

Focusing on the two focal freshwater lakes from which the ancient samples were recovered, and the adjacent marine fjord, we compared the two ancient samples to 15 present-day samples from Lake 1, 10 samples from Lake 2, and 5 present-day marine samples from Altafjord (hereafter, the 'local' population dataset). Considering just sites covered in the ancient samples and estimating genotype likelihoods to account for any uncertainty in genotypes, we find strong

covariance among present-day genomes within each lake, and likewise among genomes from the fjord (Figure 2C). The focal lakes in this study are found less than 300 metres from the fjord on land that rises steeply to the post-uplift height of 33.2 and 38.4 metres above sea-level. Isostatic rebound in northern Norway occurred rapidly over a period of several hundred years [3,14]. The rapid uplift and steepness of the terrain would produce sudden and ongoing isolation of the freshwater lakes from the marine source population. It is therefore likely that present-day stickleback in these 'isolation lakes' are descendants of early colonists that include the ancient samples. Accordingly, the strongest differentiation in allele frequencies is between genomes from Lake 1 and those from Lake 2 (PC1, $P < 0.005$), explaining 42.9% of the variance in the data (Figures 2C; Methods S1 section 2). The ancient genomes cluster most closely with the marine fjord samples, though the Lake 1 ancient sample is found between the fjord and lake samples along PC2 ($P < 0.001$; Figures 2C; Methods S1 section 2). A similar pattern is seen when considering the marine-freshwater divergent regions (Methods S1 section 2). Clustering patterns in the PCA are reflected in admixture plots, in which both ancient samples share ancestry components with the present-day fjord samples, whilst present-day lake samples retain just a lake-specific subset of this ancestral variation (Figure 2D).

The placement of the ancient samples relative to the present-day fjord and lake populations in the PCA, and the pattern of ancestry components in the admixture plots indicates high covariance in allele frequencies, consistent with strong drift associated with the colonisation of each lake population and subsequent demographic bottleneck. Such drift would genetically differentiate each lake population from the ancestral founder population, the contemporary marine population, and from one another. The PCA in Figure 2C was generated from data that excluded regions of the genome associated with parallel marine-freshwater adaptation [4], however, covariance in some locally adapted alleles could explain separation of lake and marine populations along PC2.

If the ancient samples represent the ancestral populations that first colonised the lake from the marine source population, then the ancient sample would be symmetrically related to the present-day Lake and marine fjord populations (i.e. sharing approximately equal alleles with each). To formally test this hypothesis, we computed *D*-statistics corresponding to the population history *D*(*G. nipponicus*, (ancient, (modern fjord, modern lake). To remove biases associated with coverage and post-mortem DNA damage we considered only transversions and sites covered in modern and ancient samples, randomly drawing an allele from each sample.

We focused our analyses on the Lake 2 sample, for which we had data from many unlinked genomic regions, providing jack-knife estimates of D from which to generate Z-scores. The *D*-statistic tests are consistent with the ancient sample from Lake 2 being symmetrically related to the present-day marine fjord and freshwater Lake 2 populations ($-3 < |Z| < 3$; Figure 2E). Conversely, tests assigning the ancient sample to a clade with one of the present-day sticklebacks to the exclusion of the other, *i.e.* (*G. nipponicus*, (modern, (ancient, modern))), were all rejected ($Z > 3$). Thus, based on the sharing of derived alleles (Figure 2E), the ancient stickleback from Lake 2 is inferred to have lived close to the time of the divergence of the ancestral fjord and lake populations, and prior to the strong independent drift in the two lake populations, which causes correlated allele frequencies and drives the patterns in the PCA and admixture plots (Figures 2C, and 2D).

Our findings of relative isolation and strong independent drift in the lake populations suggest reduced effective population size (N_e). This has implications for the ability of the population to adapt to freshwater, as the effectiveness with which natural selection fixes advantageous alleles in a population depends not only upon the selection coefficient (s) of an allele, but also on N_e [22]. To better understand how N_e, and by proxy, the efficacy of natural selection had varied through time we reconstructed the demographic history of fjord and lake populations using the pairwise sequentially Markovian coalescent (PSMC) method [23]. Estimates of N_e for the fjord and lake populations overlap from 100–20 KY BP, but this shared demographic history diverges from 20 to 10 KY BP (Figures 3A; Methods S1 section 3) – approximately at the directly-dated time isostatic rebound isolated the lakes from the marine population (Figure 1B). Following isolation from the marine population, we observed a steep decline in inferred N_e in both lake populations, consistent with studies of other freshwater lake populations [24].

Runs of homozygosity (ROH) provide further support for decreasing N_e in recent demographic history [25]. The impact of smaller population size of the lake stickleback results in an increased proportion of the genome being identical by descent and in long ROH, particularly in Lake 2 (Figure 3B). After excluding regions of the genome associated with parallel marine-freshwater divergence [4], the sum of ROH longer than 300 kb was significantly higher in both lake populations than in the fjord population (Wilcoxon rank sum test, $P < 0.01$). ROH sum up to 83 Mb for stickleback from Lake 1 and 277 Mb for Lake 2 (Figure S2), corresponding to 18% and 60% of the genome respectively, indicating that both populations had undergone intense genetic bottlenecks. Considering only regions associated with parallel marine-freshwater

divergence [4] (Figure S2), we find ROH clustered in known inversions and loci which show strong differentiation between fjord and lake populations (Figures S3; Methods S1 section 4), consistent with selective sweeps [26].

Our population genetic results indicate an ongoing reduction in effective population size following the colonisation of the isolation lakes. This would be expected to reduce efficacy of selection ($N_e s$) on freshwater alleles [22]. In addition to the constraints imposed by reduced effective population size, the progression of adaptation will also be dependent upon the availability of freshwater adaptive alleles upon which selection acts. Our paleogenomic data provide the first opportunity to directly compare standing genetic variation present in a freshwater lake at the start of the freshwater adaptation process to present-day genetic variation. We focused our analyses on the Lake 2 sample, for which we had data from many unlinked genomic regions associated with marine-freshwater adaptation. Using genomic positions with data present in the ancient stickleback samples, and after down-sampling present-day Lake 2 and Altafjord genomes to equivalent levels, we identified 814 regions of the genome that contain sites with strong divergence among present-day freshwater Lake 2 and marine Altafjord fish (locally divergent regions, Supplementary Information). At these locally divergent regions, the ancient stickleback from Lake 2 predominantly shared alleles with the present-day fjord population (Figure 4A). Fixed alleles in these locally divergent regions could represent instances of fixation due to drift in the lake population, rather than having a functional role in freshwater-marine adaption.

At genomic regions underlying marine versus freshwater adaptation based on the parallel divergence among a global dataset of marine and freshwater populations [4], the ancient genome also carries predominantly marine adapted genotypes, yet carries freshwater genotypes at a greater number of adaptive loci (~24%) than in the comparison between the local populations (Figure 4B). The present-day Lake 2 fish carry similar proportions of globally shared marine and freshwater genotypes to the ancient genome suggesting incomplete freshwater adaptation. Some regions of the genome enriched for the freshwater alleles in the ancient sample were also enriched for freshwater alleles in the present-day lake population (Figure 4B). However, the overall composition of the adaptive alleles carried by the present-day freshwater stickleback in Lake 2, differ from those found in the ancient genome (Figure 4B). For example, the ancient genome carries marine versions of the chromosome I inversion harbouring Na+/K+ ion transporter ATPase1a2 and the chromosome II mucin region, whereas the present-day Lake 2

stickleback carry freshwater alleles (Figure 4C). Of course, the ancient sample represents just a single individual, and the ancestral gene pool is expected to have contained a greater diversity of freshwater alleles including those found in the present-day lake stickleback. In contrast, the ancient genome carries freshwater adaptive alleles at some loci where both present-day lake and fjord populations carry marine alleles, e.g. the *GDF6* region, a major effect locus driving bony armour plate size [27], on chromosome XX (Figure 4B), 17.3Mb of chromosome IX and 9.3Mb of chromosome VIII. Therefore, it appears that some freshwater-adaptive haplotypes available as standing genetic variation during the founding of Lake 2 have subsequently been lost during the past 12,000 years.

There are clear phenotypic and genomic signatures of directional selection in the present-day populations. Stickleback sampled from Lake 1 and 2 were phenotypically low-plated, whilst stickleback sampled from the fjord were fully plated. The ectodysplasin (*EDA*) signalling pathway has a key role in the parallel evolution of the low-plated freshwater phenotype due to repeated selection of alleles derived from an ancestral low-plated haplotype [9,28,29]. There is strong evidence that these alleles persist as standing genetic variation in the marine population [4,9,12,13,30]. Consistent with the importance of *EDA* in marine-freshwater phenotypic divergence, we find differentiation between the marine fjord and lake populations (Figures S3 and S4), and evidence that both lake populations share the core freshwater haplotype at the EDA locus (Figure S4). ROH are prevalent at this locus in the two lake populations (Figure S3), consistent with a 'hard sweep' of an extended haplotype under selection in too short a time frame for recombination to restore genetic variation [26]. Inspecting the underlying genotypes, we find extended freshwater haplotypes shared among individuals within each lake, but differing between individuals in Lake 1 and Lake 2 (extending to the right and left flanks respectively, Figure S4). In both populations the ancient freshwater haplotype is flanked by marine haplotypes (Figure S4). This further highlights the independence of freshwater adaptation by stickleback in lakes just 25km apart colonised from a shared ancestral genepool.

Studies have reported compelling evidence of adaptation of Pacific threespine sticklebacks to freshwater habitats over decadal timescales [7,8], assuming that modern marine stickleback are a suitable proxy for the ancestral population. By comparing the genomes of Late Pleistocene stickleback to present day Atlantic threespine sticklebacks, we find support for this assumption, with relatively little drift in allele frequencies from the ancient to the present-day marine specimens. We also find the populations in our two study isolation lakes show clear evidence

of directional selection acting upon loci such as *EDA* which underlie marine or freshwater adapted phenotypes. These findings highlight that selection can drive adaptive alleles to high frequency at loci of large effect, even under demographic constraints. However, we do find evidence for a more stochastic process in our isolation lake populations than previously described, resulting in a freshwater optimal genotype not being reached even after several millennia. Our empirical findings are supported by forward simulations (Methods S1 section 5), in which freshwater alleles present as low frequency standing variation continue to rise to high frequency 10,000 generations after the colonisation of 'isolation lakes', with limited parallelism between lakes. Our simulations highlight that parallel adaptation is constrained by the frequency of freshwater alleles in the founding population and low migration [31], and are consistent with our coalescent estimates of changes in effective population size indicating the stochastic loss of freshwater alleles through increased drift during founder-associated population bottlenecks. The stochastic loss of freshwater-adapted alleles during colonisation of the Atlantic from the Pacific, has been proposed to have reduced parallelism in freshwater adaptation in Atlantic stickleback [32]. Our results suggest these demographic processes also occur during and after the colonisation of individual lakes, explaining observations of variation in parallelism of freshwater adaptation globally [32,33] and among geographically proximate lakes [34,35]. Thus, while the adaptation of threespine stickleback to freshwater is a highly deterministic process, we find a significant role for stochasticity in the progression of parallel adaptation.

ACKNOWLEDGEMENTS
We thank two anonymous reviewers whose comments greatly improved this manuscript. We thank Mark Ravinet, Per-Arne Amundsen and Ian Mayer for help with permitting advice. Christian Carøe for advice on extraction and library build. Mike Martin for logistical support. Lina Gislefoss and Thomas Lakeman for help with lake coring. Camilla Scharff-Olsen and Marta Ciucani for ancient DNA lab support. Mette Juul Jacobsen and Lasse Vinner of the National High-throughput DNA Sequencing Centre, University of Copenhagen, Denmark for assistance with Illumina sequencing and associated data processing of ancient samples. Enni Harjunmaa for assigning the ancient stickleback bones to their corresponding position in an X-Ray scan of a modern stickleback. Kavita Venkataramani for DNA extraction and library preparation of the modern samples. Heike Budde, Katrin Fritschi and Ilja Bezrukov for assistance with Illumina sequencing and associated data processing. Katrin Töpner for consultation for creating SLiM simulations. M.A.K. is supported by the International Max Planck Research School "From Molecules to Organisms" and the German Research Foundation (DFG). F.C.J. is supported by The Deutsche Forschungsgemeinschaft DFG SPP1819-JO1316, and the European Research Council FP7 CoG617279. A.D.F. and the ancient DNA lab work and sequencing were supported by the European Union's Horizon 2020 research and innovation programme under the Marie Skłodowska-Curie grant agreement No. 663830. The geological field work was funded jointly by NGU and the archaeological research project "Stone Age Demographics" at the University of Tromsø.

Author contributions: A.D.F. conceived and coordinated the study. Collection of sediment cores and all geological analyses were conducted by A.R. Modern sticklebacks were sampled in the field by A.F. Ancient DNA lab work was conducted by A.D.F. and M.T.P.G. Modern DNA lab work was conducted by M.K. and F.C.J. Genomic data analyses were conducted by M.K., F.C.J. and A.D.F. M.K. and A.D.F. drafted the initial manuscript with all authors contributing towards the writing of this paper.

Declaration of interests:
The authors declare no competing interests.

Figure 1. The ecological and geological context of Late Pleistocene stickleback remains.

(**A**) Ancient and present-day samples were collected from Klubbvatnet freshwater lake (70° 36´ N, 23° 37´ E; hereafter Lake 1), and from Jossavannet freshwater lake (70° 27´ N, 23° 47´ E; hereafter Lake 2), additionally samples of the marine ecotype were collected from the outer branch area (next to the lake sites) of Altafjord (70° 27´ N, 23° 46´ E). (**B**) The ancient samples were found in the sediment layers of cores from the two lakes corresponding to the isolation phase, dated to ~11.8 and 12.9 KY BP respectively. An example of the variation in core stratigraphy is shown on the left, schematic diagrams of the stratigraphy in the two study lakes are shown to the right. (**C**) Bones, spines and bony armour plates found in Lake 2. The background grid is mm-scale. Bone positions illustrated on an X-ray scan of modern freshwater fish (above). See Figure S1 for details.

Figure 2. Relationships between ancient and present-day stickleback.
Principal component analyses (PCA) of the global dataset from Jones *et al.* [4], a single modern sample from each of Altafjord, Lake 1 and Lake 2 and ancient samples from Lake 1 and Lake 2, based on (**A**) transversions in non-divergent regions, (**B**) transversions in freshwater-marine divergent regions identified by Jones *et al.* [4]. (**C**) PCA of local present-day and ancient samples using transversions in non-divergent regions. (**D**) Admixture plots of combined global and local populations. (**E**) *D*-statistics of the form (Lake 2, Altafjord; ancient, Japan Sea stickleback) testing whether the ancient sample shares more alleles with the present-day lake or fjord samples. The results were not significantly different from zero ($-3 < |Z| < 3$), suggesting the ancient sample is symmetrically related to both. Red markers show D-statistics (top axis) and horizontal bars show associated standard error. Black markers show Z-scores (bottom axis). D-statistics therefore support the topology shown in the schematic.

Figure 3. Demographic history of local marine and freshwater stickleback.
(**A**) PSMC estimates of changes in effective population size (N_e) over time inferred from the autosomes of a Lake 1 (yellow), Lake 2 (blue) and Altafjord (orange) sample. Thick lines represent the median and thin light lines of the same colour correspond to 100 rounds of bootstrapping. (**B**) Distribution of the length of runs of homozygosity (ROH) greater than 0.3 Mb in the genomes of five samples each from Lake 1 (yellow), Lake 2 (blue) and Altafjord (orange). The thick black line shows the median. The bottom and top of the box represent the 1st (Q1) and 3rd (Q3) quartile. The upper whisker corresponds to the smaller value of the maximum length of ROH or the sum of Q3 and 1.5 times the size of the box (Q3-Q1). All values above the upper whisker are shown as black circles. The lower whisker shows the smallest length of ROH for the corresponding individual. The PSMC and ROH analyses exclude known freshwater-marine divergent and 100kb flanking regions.

Figure 4. Marine versus freshwater adaptive alleles in the ancient and modern samples
(**A**) The probability of 'Lake 2 ancestry' in the ancient sample is plotted for 814 locally divergent regions of the genome (windows containing variant(s) with fixed allele frequency difference among 5 fish from each of Altafjord and Lake 2). Windows are plotted from left to right according to the probability of freshwater ancestry in the ancient genome. For each genomic region, the mapDamage-rescaled base qualities are plotted in grey-scale for the ancient genome. The probability of freshwater ancestry in

five fish from each of present-day Altafjord and Lake 2 populations respectively are shown above and below the ancient genome probabilities. (**B**) The probability of freshwater ancestry in the ancient genome is plotted for 34 genomic regions underlying marine versus freshwater adaptation. These regions were identified based on parallel divergence among global marine versus freshwater populations using cluster separation score (CSS) [4]. Regions of the genome are plotted from left to right according to the probability of freshwater ancestry in the ancient genome. For each genomic region, the mean mapDamage-rescaled base qualities are plotted in grey-scale below the corresponding probability scores for the ancient genome. The probability of freshwater ancestry in the present day Altafjord and Lake 2 populations are respectively shown above and below the ancient genome probabilities. (**C**) Underlying genotypes at a focal subset of adaptive loci. Rows represent individual fish; columns represent individual single nucleotide polymorphisms; red boxes indicate marine alleles; blue boxes indicate freshwater alleles; grey boxes are missing data. The mean mapDamage-rescaled base qualities are plotted in grey-scale below the corresponding ancient genome probabilities for each site. Transversions, which are less prone to DNA damage, are marked by grey triangles.

STAR METHODS

RESOURCE AVAILABILITY

Lead Contact

Further information and requests for resources, material and reagents should be addressed and will be fulfilled by the lead contact, Andrew Foote (andrew.foote@ntnu.no).

Materials Availability

Raw sequence data and BioSample details are available at the National Centre for Biotechnology Information (NCBI) under BioProject accession number: PRJNA693136.

Data and Code Availability

The accession number for the genomic data generated for this study is NCBI: PRJNA693136 Previously published genomic data of 20 global samples from Jones *et al.* [4] were downloaded from NCBI in SRA format (SAMN00627549-SAMN00627550; SAMN00627914 - SAMN00630301). The code used in this study is listed in the Key Resources Table and at https://github.com/Stickle-Back-in-Time.

EXPERIMENTAL MODEL AND SUBJECT DETAILS

Ancient sample collection and geological analysis

Sediment core samples from a number of lakes in the Finnmark region were collected in late spring 2018 and 2019, as part of a study on postglacial relative sea-level changes. Both of the lakes presented in this paper, are relatively shallow and were cored with a "Russian-type" peat corer [36]. The one metre-long, half-cylinder-shaped samples of lake deposits were collected and transported to the laboratory. As part of the sediment analysis, bulk samples of core material were carefully subsampled and wet-sieved at 125-µm for analysis of macroscopic remains of biota. During basin isolation from the sea, fundamental environmental changes lead to a complete replacement of floral and faunal assemblages, which is apparent in sediment core biostratigraphy [14]. Marine to lacustrine transitions are often visually distinct as laminated facies and can usually be further determined to within a few centimeters, using preserved remains from certain marine, brackish and freshwater organisms. One such organism which has often been found indicative of a lake in the isolation phase is the three-spine stickleback [14,37,38,39]. When found, stickleback bones were carefully picked out from the wet-sieved residual material, cleaned and dried at low temperature, before being sent for biological analysis.

Marine-lacustrine transitions were identified using biostratigraphy [14], before sediment cores were subsampled for material suitable for radiocarbon dating. 1-cm-thick slices of the core were wet-sieved and residual terrestrial plant remains were identified, picked and dried overnight before being submitted to the Poznan Radiocarbon Laboratory, Poland. For Klubbvatnet, this comprised one sample (Lab no Poz-111167) of seeds (not identified to species), a small twig and some mosses, weighing in total 12 mg, yielded a radiocarbon age of 10140 +/- 50 years, which corresponds to a calendar age interval of 12040-11410 cal yr BP (2 sigma). For Jossavannet, a series of four samples were dated across the transition. Most importantly, a

sample of Salix leaves (Poz-115352, 7 mg) picked at the boundary yielded 11080 +/- 50 radiocarbon yrs, calibrated to 13070-12800 cal yr BP. This is supported by a marine sample of algae found 7 cm deeper (large sample Pox-115492, weighing 61 mg), which yielded 11780 +/- 50, calibrated to 13330-13070 cal yr BP. It is further supported by a third sample of Salix leaves (Poz-115350, 5 mg) found shortly above the transition, yielding 11420 +/- 50, calibrated to 12920-12700 cal yr BP. All calibration using OxCal software with IntCal.

Modern sample collection

Adult threespine stickleback specimens were collected using minnow traps from the two lakes from which our ancient stickleback samples originated: fifteen individuals from the 1600 m^2 Klubbvatnet freshwater lake above the village of Neverfjord (70° 36′ N, 23° 37′ E; Lake 1), and ten individuals from 9800 m^2 Jossavannet freshwater lake (70° 27′ N, 23° 47′ E; Lake 2). Additionally, five samples of the marine ecotype were collected from the outer branch area (next to the lake sites) of Altafjord (70° 27′ N, 23° 46′ E). Samples were collected under permit (201300202-62) from Finnmark Fylkeskommune. Upon sampling, stickleback were euthanized and stored in 95% ethanol.

METHOD DETAILS

DNA extraction

Lab work was performed at the Friedrich Miescher Laboratory of the Max Planck Society in Tübingen. Fin clips of the collected sticklebacks were used for standard Proteinase K digestion (New England Biolabs GmbH, Frankfurt am Main, Germany). Each sample was first incubated for 5 hours at 58°C in 400 µl lysis buffer (50mM Tris-HCl pH=8, 0.1M NaCl, 10mM EDTA pH=8, 0.8% SDS, 15 µg proteinase K) and for 30 min at 37°C with additional 2 µg RNAse A. After adding 150 µl 5M potassium acetate, the sample was stored at 4°C overnight and centrifuged at 4000 rpm for 30 min. Extracted DNA was purified from the supernatant via AmpureXP bead purification (Beckman Coulter GmbH, Krefeld, Germany).

Nextera library preparation was performed with assembled Tn5 bound to magnetic beads. 5 ml of Hydrophilic Streptavidin Magnetic Beads (NEB) were transferred into a falcon tube, placed on a magnet and the bead-storage buffer was removed. The beads were washed with 20 ml streptavidin binding buffer (0.6 M NaCl, 10 mM Tris pH=8.0, 0.5 mM EDTA, 0.1% Triton X-100). Afterwards 30 ml streptavidin binding buffer as well as 400 µl assembled Tn5 were added to the magnetic beads. The mixture was inverted and rotated at 10 rpm at RT for 30 min. The

falcon tube was again placed on the magnet, the buffer was removed and replaced by 30 ml of Dialysis buffer (50 mM HEPES-KOH pH 7.2, 0.2 M NaCl, 0.2 mM EDTA, 2 mM DTT, 0.2% Triton X-100, 20% glycerol). The suspension was rotated for another 5 min at 10 rpm, the buffer was removed and 20 ml Dialysis buffer were added for storage of Tn5-on-beads.
2 µl extracted DNA was used for tagmentation with 10 µl Tn5-on-beads in 1x TAPS-DMF buffer (10 mM TAPS, 5 mM $MgCl_2$, 10% DMF) for 15 min at 55°C (total volume 20 µl). 50 µl SDS wash buffer (10 mM Tris pH=8, 30 mM NaCl, 0.1% Triton X-100, 0.3% SDS) were added to the tagmented product for SDS stripping and the suspension was incubated at 55°C for further 4 min. To remove SDS, the samples were placed on a magnet, the supernatant was removed and the tagmented DNA bound to the beads was washed twice with wash buffer (10 mM Tris pH=8, 30 mM NaCl, 0.1% Triton X-100).The library was dual indexed and amplified in a 9-cycle PCR using Q5 High Fidelity Polymerase (Biolabs New England). 50 µl PCR-Mastermix (200uM dNTPs, 300uM of each nextera primer, 1 U Q5 High Fidelity Polymerase, 1x Q5 buffer) was therefore added to each sample. PCR temperature profile included an initial step at 72°C for 5 min to fill up the 9 basepair long gaps made by Tn5 during the tagmentation, an activation step at 98°C for 30 s, followed by 9 cycles of denaturation at 98°C for 15 s, annealing at 65°C for 20 s and elongation at 72°C for 90 s. Amplified DNA was then purified with AmpureXP bead purification (Beckman Coulter GmbH, Krefeld, Germany).

Ancient DNA lab work

Ancient DNA lab work was conducted at the dedicated ancient DNA facilities at the Centre for GeoGenetics, University of Copenhagen. DNA was extracted using a silica-based method, where each individual bone or spine was incubated overnight under motion at 55°C in 500 µl extraction buffer (0.45 M EDTA, 0.1 M UREA, 100 µg proteinase K). Each sample was then centrifuged at 2300 rpm for 5 min and the supernatant was collected and concentrated and purified using a Zymo-Spin V reservoir (Zymo Research Irvine, CA, USA) and Qiagen MinElute spin column (Qiagen, Inc., Valencia, CA, USA). To maximise library complexity by reducing the number of DNA purification steps during library preparation, an Illumina library was constructed using the blunt-end single tube (B.E.S.T.) method [40]. The library was dual indexed and amplified in either a 15-cycle (Lake1 sample) or 20-cycle (Lake 2 sample) PCR using AmpliTaq Gold (ThermoFisher Scientific). The 50ul PCR reaction contained 15ul of library, 25uM dNTP, 1x PCR buffer, 2.5 mM $MgCl_2$, and was made up to 50ul with molecular grade water. PCR temperature profile included an activation step at 95°C for 5 min, followed by 15/20 cycles (sample dependent: lake1/lake2) of denaturation at 95°C for 30 s, annealing at

55°C for 30 s and elongation at 72°C for 1 min, with a final extension step at 72°C for 7 min. PCR products were then purified using Agencourt AMPure XP beads (BeckmanCoulter). The dual index amplified library of the Lake 1 sample had mean insert size of 186bp, including 114bp of index and adapters, indicating mean DNA fragment size of 72bp. Peak molarity was 286 pmol/l, comprising 34% of the library (including adapter dimer, lower and upper size markers) as quantified using an Agilent 2200 TapeStation instrument with D1000 High Sensitivity ScreenTape and reagents. The dual index amplified library of the Lake 2 sample had mean insert size of 186bp, including 114bp of index and adapters, indicating mean DNA fragment size of 72bp. Peak molarity was 26,100 pmol/l, comprising 85% of the library (including lower and upper size marker peaks). Extraction, library build and index PCR blanks were also included to evaluate potential contamination during the library building process. To achieve the minimum threshold for DNA molarity, the Lake 1 DNA library was then pooled with an ancient killer whale *Orcinus orca* DNA library and sequenced across two lanes of 80bp-SE sequencing of an Illumina HiSeq4000, and the Lake 2 library was run across an entire single lane of 80bp-SE sequencing of an Illumina HiSeq4000 at the Danish National High-throughput Sequencing Centre of Copenhagen University (seqcenter.ku.dk).

Mapping, filtering and masking

Sequencing data from modern samples generated for this study were demultiplexed and adapters removed using bcl2fastq. Sequencing data of 20 global samples (Bear Paw Lake sample was excluded as this was also the reference sample) from Jones *et al.* [4] were downloaded from NCBI in SRA format (SAMN00627549-SAMN00627550; SAMN00627914 - SAMN00630301). SRA files were transformed to fastq files by using fastq-dump. Sequencing of the ancient samples resulted in 1,381,302 reads for Lake 1 and 627,366,889 million reads for Lake 2. AdapterRemoval [41] removed adapters from the single-end reads of the ancient samples of Lake 1 and Lake 2 and trimmed both Ns and low-quality bases from the reads. The generated fastq files of the 20 global samples, as well as trimmed sequencing data of both ancient samples, were aligned against the reference genome gasAcu1 [4] by using the Burrows-Wheeler Alignment Tool (BWA) with the aln algorithm [42], disabling seeding (option'-l 1024) to turn-off seeding thereby increasing mapped data by including reads with post mortem damage at the read ends [43]. Based on the proportion of mapped and unmapped reads, endogenous content was estimated at approximately 2-4% for each sample. Sequencing data aligned to the stickleback reference genome encompasses 9,127 reads for the ancient sample from Lake 1 and 7,199,676 reads for the ancient sample from Lake 2, corresponding to coverage of ≥1× at 369,344 bp and

16,923,179 bp from the Lake 1 and Lake 2 ancient samples respectively. The resulting bam files were sorted and merged by Samtools [44]. Sequencing data of all modern samples were subsequently aligned against the reference genome gasAcu1 [4] using the BWA mem algorithm [42], mean coverage for each sample is given in table S1. Generated bam files were then sorted by Samtools [44]. All types of duplicates in all sorted bam files were identified by MarkDuplicates from Picard Tools [http://broadinstitute.github.io /picard/]. Masked regions as well as the sex chromosome (chrXIX) were removed from the bam files. Masked regions encompassed interspersed repeats and low complexity DNA sequences detected by RepeatMasker [45] covering 3.72% of the stickleback genome as well as highly repetitive DNA sequences detected by WindowMasker [46] from the NCBI C++ toolkit covering 25.59% of the stickleback genome using -sdust true as setting. After removing duplicates and masked regions, 5,054 reads were left for the ancient sample of Lake 1 and 329,226 reads for Lake 2.

QUANTIFICATION AND STATISTICAL ANALYSIS

Assessing postmortem DNA damage and contamination

Analyses of potential nucleotide misincorporations using PMDtools [47] to compare with the modern reference genome revealed that sequencing reads exhibited characteristic post-mortem damage patterns [15,48], specifically an excess of C→T transitions at the 5′ termini as expected from deamination, and the complementary G→A transitions at the 3′ termini. Therefore, except where otherwise stated, only transversions were considered in downstream analyses that included the ancient samples. Contamination from present-day DNA can be estimated from the number of heterozygous calls in haploid markers [49]. As both our ancient stickleback were females (see below), contamination could only be inferred from the mitochondrial genomes. Coverage was 1x across most sites, and we detected no heterozygous genotypes in either fish. Furthermore, all segregating sites conformed to the expected haplotype structure based on comparison with modern samples in the same clade. Taken together with the high proportion of reads with DNA damage patterns at the read ends, these results suggest our genome data represented endogenous DNA from the ancient stickleback bones.

Sexing

Sticklebacks have an XY sex-determination system, where males are the heterogametic sex. Males are therefore haploid for the X chromosome and diploid for the autosomes, while females are diploid for both the X chromosome and autosomes. The sex of the ancient samples was determined by comparing the mean coverage of the autosomes (excluding unassembled

scaffolds), the pseudoautosomal region (chrXIX:1-3300000 and chrXIX:12270000-20240660), and the sex-determining region (chrXIX:3300000-12270000) among 4 female and 4 male modern genomes down-sampled to comparable coverage with each ancient genome. Both ancient samples had approximately equivalent coverage across all three regions implying that both are diploid for the sex-determining region of the X chromosome, i.e. are female (Methods S1 section 6). For each modern individual the down-sampling was repeated 10 times with different random seeds to initiate the down-sampling.

Principal Component Analysis

We used pseudo-haploid genotype calls of globally distributed modern marine and freshwater genomes [4] and the ancient samples. First, we sampled autosomal regions outside of known freshwater-marine divergence associated regions as identified by Jones *et al.* [4] to compare across geographically informative markers. Then, we compared covariance within freshwater-marine divergence associated regions among samples using ecology informative markers. The ancient samples were included in the PC computations and not projected onto PCs of modern samples, which has the advantage of providing a quality control measure. For example, if the ancient samples were impacted by sequencing- or sequence data processing errors, the samples would appear as outliers in the PCA. Instead they cluster with Atlantic and marine samples respectively in the first two PCA plots (Figure 2A). In the first PCA, both ancient samples were at the extreme edge of PC1 showing closest affinity to the Atlantic samples. Inclusion of a single randomly selected modern sample from Altafjord, Lake 1 and Lake 2 showed that the modern samples also cluster at the edge of PC1 (Figure 2A). This suggests structure among the Atlantic samples, potentially reflecting past biogeographical processes [50] and gene flow during the Holocene between Pacific and Atlantic lineages, rather than artefacts of unmasked DNA damage or missingness of the data in the ancient samples. In Figure 2A, PC1 clearly separates out Atlantic from Pacific samples, with no sub-clustering of California samples, suggesting the signal was driven by the inclusion of multiple samples adjacent populations. Additional filtering steps included in these analyses were the removal of regions of poor mapping quality ($Q < 30$), removal of sites with low base quality scores ($q < 20$), calling only SNPs inferred with a likelihood ratio test (LRT) of $P < 0.000001$, a minimum allele frequency of 0.05 so that alleles had to be called in a minimum of two individuals, discarding reads that did not map uniquely, adjusting q-scores around indels, adjusting mapping quality to 50 for excessive mismatches, discarding bad reads (flag >=256), and the removal of transitions to avoid bias from C⬭T and A⬭G DNA damage patterns. The eigenvectors from the covariance matrix were generated with

the R function "eigen", and significance was determined with a Tracy-Widom test [51] performed in the R-package AssocTest [52] to evaluate the statistical significance of each principal component.

The relationship of the 30 modern samples collected from the two lakes and fjord in Finnmark, and the two ancient samples was explored using PCAngsd, a Principal Component Analysis for low depth next-generation sequencing data using genotype likelihoods, thereby accounting for the uncertainty in the called genotypes which is inherently present in low-depth sequencing data [53]. We restricted the analyses to transversions covered in at least one of the two ancient samples, which restricted the dataset to 2,267 SNPs in autosomal chromosomes and outside of freshwater-marine divergent regions. Over 90% of the included SNPs were >100,000 bp apart, thus reducing autocorrelation in covariance due to linkage disequilibrium. Filtering steps were as specified above. The statistical significance of each principal component was estimated from the eigenvalues as above.

Individual Assignment and Admixture Analyses

An individual-based assignment test was performed using NGSadmix [54], a maximum likelihood method that bases its inference on genotype likelihoods. The input genotype likelihood values were the same as those use above for PCAngsd, as were the filtering steps. NGSadmix was run with the number of ancestral populations K set from 2–10. For each of these K values, NGSadmix was re-run five times for each value of K, and with different seeds to ensure convergence. The uppermost hierarchical level of structure, inferred from the greatest step-wise increase in log likelihood, ΔK [55], identified two clusters. PCA and individual assignment-admixture models draw inference from similar information and therefore generate similar axes of variation [56,57]. Both methods typically identify the samples with the greatest population-specific drift that therefore share derived alleles that were rare in the source populations or have lost ancestral alleles from standing variation, as the major axes of structure [56]. Accordingly, both PCAngsd and NGSadmix identified the uppermost hierarchical level of structure within our data set as being between the Lake 1 and Lake 2 with other samples sharing ancestry with both. However, the ΔK method is prone to over- or under-estimating population genetic structure [58] and performs poorly under scenarios with migration among populations at inferring hierarchical population structure [59]. Changes in likelihoods show the biggest jumps between K=2 and K=3, and between K=3 and K=4, before plateauing to a gradual rising rate in likelihood. Likelihood estimates for K=3 and K=4 were also highly consistent, having the

lowest standard deviations. We therefore present the admixture plots for *K*=3 and *K*=4 in Figure 2D.

***D*-statistics**

To investigate whether pairs of modern stickleback populations evenly shared derived alleles with the ancient samples, we estimated D-statistics. The test can be used to evaluate if the data are inconsistent with the null hypothesis that the tree (((Lake, Fjord), ancient), outgroup) is correct.

The D-statistic is based on counts of derived alleles shared by the ancient sample and the modern marine sample, but not the modern freshwater sample; and comparing this with counts of derived alleles shared by the ancient sample and the modern freshwater sample, but not the modern marine sample. We find the ancient sample shares a roughly equal number of derived alleles with both the modern marine and freshwater samples. This statistic excluded the known freshwater-marine divergent regions of the genome. The D-statistic is insensitive to drift in allele frequencies and is a test of 'treeness'. Our hypothesis is that the ancient sample represents an individual from the time that the ancestors of the present-day lake and present-day marine samples split. We can express this hypothetical relationship in newick format as (ancient, (lake, fjord)).

No mutations that occur along the branches to the lake or the fjord samples will count towards the D-statistic as these will not be shared with the ancient sample. Under neutral expectations, changes in allele frequencies should be random and the standing variation present in the ancient sample should be shared equally, when sampling a random allele from each SNP. We find this to be the case and the statistic is confirmation of the tree-like relationship above. We represent this tree in newick format as (outgroup, (ancient, (fjord, lake))).

If our hypothesised demographic history was incorrect, possible alternative topologies would be: (outgroup,(fjord,(ancient, lake))) or (outgroup,(lake,(ancient, fjord))). If one of these topologies were the true demographic history the ancient sample would share an excess of derived alleles with the lake population (left-topology) or the fjord population (right-topology). However, these topologies were rejected (-3 > Z > 3).

The definition used here is from Durand, Patterson, Reich, and Slatkin [60]:

$$D = \frac{\mathrm{nABBA} - \mathrm{nBABA}}{(\mathrm{nABBA} + \mathrm{nBABA})}$$

where in the tree given above, nABBA is the number of sites where lake and ancient samples share a derived allele, and the fjord samples has the ancestral allele; and nBABA is the number of sites where the fjord and ancient samples share a derived allele, and the lake sample has the ancestral allele. Under the null hypothesis that the given topology is the true topology, we expect an approximately equal proportion of ABBA and BABA sites and thus D = 0. The significance of the deviation from 0 was assessed using Z-scores, which are based on the assumption that the D-statistic (under the null hypothesis) is normally distributed with mean 0 and a standard error achieved using the jackknife procedure. The tests were implemented in ANGSD [61] and performed by sampling a single base at each position of the genome to remove bias caused by differences in sequencing depth at any genomic position, removing transitions to avoid bias from C⬭T and A⬭G DNA damage patterns, and only considering sites covered in the ancient sample (only the Lake 2 sample was included). Further filtering steps were as specified above for PCA and excluding regions known to be associated with marine-freshwater divergence. The Japan Sea stickleback *Gasterosteus nipponicus* (NCBI: PRJDB5176) was used as the outgroup.

Mitochondrial DNA analysis

Both ancient samples were found to be female based on comparable read coverage across the autosomal, pseudo-autosomal and sex determining regions of the X-chromosome. Therefore, we reconstructed the mitochondrial DNA phylogeny to test whether the ancient samples were directly matrilineally ancestral to either local marine or freshwater populations (Methods S1 section 6). The alignment of the mitogenomes of the 81 individuals included in the study by Liu *et al.* [24] was accessed via the dryad repository https://doi.org/10.5061/dryad.46fb1. Modern genomic data from our two lake and fjord study sites were then mapped to the de novo reference mitogenome sequence generated by [24], which excluded the control region due to the high number of indels. Mapping criteria were the same as for the nuclear genome. We then assembled a consensus sequence of the mitochondrial genome of each ancient sample, manually inspecting mapped reads and removing those which had a T within 30 bp of the 5′ end where all other sequences had a C at the same site, and similarly removing those which had an A within 30 bp of the 3′ end where all other sequences had a G at the same site. As per Liu *et al.* [24], the mitogenome of *G. wheatlandi* (GenBank Accession no. AB445129) was added as an outgroup and a Maximum Likelihood tree was constructed using PHYML 3.0 [62], applying the same settings as Liu *et al.* [24], *i.e.* GTR model for substitution, allowing variable proportions of invariable sites and mutation rates across sites (GTR + I + gamma) and using 100 bootstraps.

The present-day freshwater sticklebacks formed two monophyletic clades corresponding to samples from Lake 1, and those from Lake 2, indicating a recent common maternal ancestor within each lake, and no detectable immigration into either lake (Methods S1 section 6). Mitochondrial genomes generated from the present-day marine samples collected from Altafjord, and the ancient samples also fell within the clade representing the so-called 'European Lineage' [63], but were intermixed among sequences from Denmark, Germany, Greenland and southern Norway. Thus, the ancient samples did not represent the direct mitochondrial ancestor of the local present-day freshwater population within the same lake. However, mitochondrial DNA represents a single genealogy and the ancient is a single sample, and the high haplotype diversity in our Altafjord sample set, and the lack of fine-scale phylogeographic patterns, suggests the ancestral marine founders of each lake population may have had similarly high mtDNA haplotype diversity.

Pairwise sequentially Markovian coalescent

The PSMC model estimates the Time to Most Recent Common Ancestor (TMRCA) of segmental blocks of the genome and uses information from the rates of the coalescent events to infer N_e at a given time, thereby providing a direct estimate of the past demographic changes of a population [23]. We selected the highest coverage modern genomes, building a consensus sequence of each bam file in fastq format sequentially using: firstly, SAMtools mpileup command with the –C50 option to reduce the effect of reads with excessive mismatches; secondly, bcftools view –c to call variants; lastly, vcfutils.pl vcf2fq to convert the vcf file of called variants to fastq format with further filtering to remove sites with less than a third or more than double the average depth of coverage and Phred quality scores less than 30. Furthermore, we excluded marine-freshwater divergence associated regions and 100 kb flanking either end. The PSMC inference was then carried out using the recommended input parameters as previously applied to threespine stickleback genomes [24], i.e. 25 iterations, with maximum TMRCA (Tmax) = 15, number of atomic time intervals (n) = 64 (following the pattern (1*4 + 25*2 + 1*4 + 1*6), and initial theta ratio (r) =5. Plots were scaled to real time as per [24], assuming a generation time of 2 years and a neutral autosomal mutation rate of 3.7×10^{-8} substitutions/nucleotide/generation. To check for variance in N_e across the genome, we performed 100 bootstrap replicates, conducted by randomly sampling with replacement 5-Mb sequence segments obtained from the consensus genome sequence. To be assured that the inferred demographic history is not impacted by the sequence coverage, sequencing data of

freshwater stickleback BS65 from Feulner *et al.* [64] was processed identically to our samples and downsampled to different coverages (Methods S1 section 3). The PSMC plot of these samples shows a consistent reduction in N_e for all samples, which suggests that lower coverage can affect the quantitative estimate of N_e, but not the overall pattern. In humans, PSMC has reduced power to estimate N_e for time periods less than 20 KYA from human genomes with an assumed generation time of 25 years, due to too few recombination events in the sequence representing this time interval [23]. We found that stickleback genomes, for which generation time is an order of magnitude lower, resulted in highly consistent PSMC bootstrap plots up to 2 KYA; representing an equivalent number of generations to that found for humans for which PSMC can accurately estimate ancestral N_e. Thus, PSMC has sufficient power to estimate changes in N_e up to, and after the colonisation of each of our study lakes and throughout most of the Holocene.

Runs of homozygosity

Runs of homozygous genotypes (ROH) were identified using the window-based approach implemented in PLINK v1.07 [65] from an input file of genotype likelihoods generated by ANGSD [61] with the following filtering settings: removing reads of poor mapping quality (MAPQ < 30), removing sites with low base quality scores (q < 20), calling only SNPs inferred with a likelihood ratio test of P < 0.000001, discarding reads that did not map uniquely, adjusting q-scores around indels, adjusting minimum quality score to 50 for excessive mismatches, and discarding bad reads (flag >=256). We estimated ROH from pruned and unpruned data and found minimal qualitative difference with our data. Sliding window size was set to 300 kb, with a minimum of 50 SNPs at a minimum density of 1 SNP per 50 kb required to call a ROH. To account for genotyping errors, we allowed up to 4 heterozygote sites per 300 kb window within called ROHs, as per ref. [66]. A length of 1,000 kb between two SNPs was required in order them to be considered in two different ROHs.

***F*ST statistics**

F_{ST} statistics between two populations at a time were performed with vcftools [67] from an input file in variant call format (VCF) created by bcftools mpileup and bcftools call [44,68]. The reference stickleback genome gasAcu1 [4] and modern samples sequenced at high coverage with five samples from each location were used as input for bcftools mpileup. The output file was subsequently piped into bcftools call which used the multiallelic-caller to output a VCF file for all fifteen modern samples. Thereafter, the resulting VCF file was used for calculating F_{ST}

estimate per site between each two populations based on Weir and Cockerham's method [69] by using vcftools. The F_{ST} estimate was processed in *R* [70] and plotted in 10kb sliding windows with 5kb steps in figures S8-10. For figure S11, the goal was to visualise variation at a finer-scale, we therefore opted to estimate F_{ST} per site. The VCF file was filtered with vcftools for sites with a minor allele frequency greater than or equal to 0.07, at least 80% of the data non-missing, a quality value above 30, and mean depth values as well as genotypes with a depth between 2 and 9 excluding indels. Subsequently, F_{ST} was estimated per site [71], and plotted in R using Friedman's 'super smoother' with a span of 1/50 [72,73] (Methods S1 section 4).

Comparison of ancient and modern genotypes

In order to investigate the marine and/or freshwater origin of adaptive alleles carried by the ancient genome we assigned the ancestral state of each allele, conditioning on allele frequencies in either geographically-proximate present-day marine and freshwater populations (Lake2, freshwater; Altafjord, marine; "locally divergent"), or on parallel-divergent marine and freshwater populations from throughout the Northern Hemisphere species range ([4]; "globally divergent"). We estimated genotype probabilities only for the Lake 2 ancient sample for which there was sufficient coverage in known freshwater-marine adaptive regions. To maximize the available data we rescaled base quality scores using mapDamage 2.0 [74], which penalizes the quality score of bases likely to be impacted by post-mortem damage based on the posterior distribution of damage-associated parameters, thereby allowing the inclusion of transitions (with a measure of confidence in the inference drawn from individual bases).

We started by identifying regions of the genome that show signs of elevated divergence among marine and freshwater populations, that therefore contain ancestry-informative variants. First, we focused on regions that were differentiated between the local Lake 2 and Altafjord present-day populations by down-sampling the five highest coverage modern samples from each of Lake 2 and Altafjord to equivalent coverage to the ancient sample. We then identified variants with fixed differences between these two modern populations. 813 genomic windows that contained data from the ancient genome sample and had variants with strong divergence in allele frequency among local geographic populations were identified first by taking 100kb of flanking sequence either side of SNPs with fixed frequency differences and then merging overlapping windows. A similar approach was used to identify 34 windows of global parallel marine-freshwater divergence. Within each window, for each of the locally-divergent and globally-divergent analyses, we used ancestry-informative SNPs (those with allele frequency

differences >=0.8 between the geographically-local or global marine and freshwater populations) to calculate the probability of the ancient genome having either 'freshwater' or 'marine' ancestry, and averaged the value for each window.

Specifically, we defined two possible ancestries for the ancient genome A_{marine} and A_{fresh}
Where the allele carried by the ancient genome shares most recent common ancestry with other marine and freshwater fish respectively. The probability of observing an allele (0,1) in the ancient genome given a specific ancestral state can therefore be calculated as:

Pr(allele|Ancestry):
$P(0|A_{marine}) = f_{marine}(0)$
$P(1|A_{marine}) = f_{marine}(1)$
$P(0|A_{fresh}) = f_{fresh}(0)$
$P(1|A_{fresh}) = f_{fresh}(1)$

We assume uniform prior probabilites $P(A_{marine})$ and $P(A_{fresh})$, and calculate the posterior probability of each possible ancestral state as:

$$\mathrm{P}(Ancestry|allele) = \frac{P(allele|Ancestry)P(A)}{\sum_i P(Ancestry_i|allele)}$$

ADDITIONAL RESOURCES

Our study has not generated or contributed to a new website/forum and it is not part of a clinical trial.

References

1. Dehasque, M., Ávila- Arcos, M.C., Díez- del- Molino, D., Fumagalli, M., Guschanski, K., Lorenzen, E.D., Malaspinas, A., Marques- Bonet, T., Martin, M.D., Murray, G.G.R., *et al.* (2020). Inference of natural selection from ancient DNA. Evol Lett *4*, 94–108.

2. Morris, M.R.J., Bowles, E., Allen, B.E., Jamniczky, H.A., and Rogers, S.M. (2018). Contemporary ancestor? Adaptive divergence from standing genetic variation in Pacific marine threespine stickleback. BMC Evolutionary Biology *18*, 113.

3. Romundset, A., Bondevik, S., and Bennike, O. (2011). Postglacial uplift and relative sea level changes in Finnmark, northern Norway. Quaternary Science Reviews *19–20*, 2398–2421.

4. Jones, F.C., Grabherr, M.G., Chan, Y.F., Russell, P., Mauceli, E., Johnson, J., Swofford, R., Pirun, M., Zody, M.C., White, S., *et al.* (2012). The genomic basis of adaptive evolution in threespine sticklebacks. Nature *484*, 55–61.

5. Bell, M.A., and Foster, S.A. (1994). The Evolutionary Biology of the Threespine Stickleback (Oxford University Press).

6. Peichel, C.L., and Marques, D.A. (2017). The genetic and molecular architecture of phenotypic diversity in sticklebacks. Phil. Trans. R. Soc. B *372*, 20150486.

7. Lescak, E.A., Bassham, S.L., Catchen, J., Gelmond, O., Sherbick, M.L., von Hippel, F.A., and Cresko, W.A. (2015). Evolution of stickleback in 50 years on earthquake-uplifted islands. Proc Natl Acad Sci USA *112*, E7204–E7212.

8. Bell, M.A., Aguirre, W.E., and Buck, N.J. (2004). Twelve Years of Contemporary Armor Evolution in a Threespine Stickleback Population. Evolution *58*, 814–824.

9. Colosimo, P.F., Hosemann, K.E., Balabhadra, S., Villarreal, G., Dickson, M., Grimwood, J., Schmutz, J., Myers, R.M., Schluter, D., and Kingsley, D.M. (2005). Widespread Parallel Evolution in Sticklebacks by Repeated Fixation of Ectodysplasin Alleles. Science *307*, 1928–1933.

10. Bassham, S., Catchen, J., Lescak, E., von Hippel, F.A., and Cresko, W.A. (2018). Repeated Selection of Alternatively Adapted Haplotypes Creates Sweeping Genomic Remodeling in Stickleback. Genetics *209*, 921–939.

11. Nelson, T.C., and Cresko, W.A. (2018). Ancient genomic variation underlies repeated ecological adaptation in young stickleback populations. Evolution Letters *2*, 9–21.

12. Schluter, D., and Conte, G.L. (2009). Genetics and ecological speciation. PNAS *106*, 9955–9962.

13. Roesti, M., Gavrilets, S., Hendry, A.P., Salzburger, W., and Berner, D. (2014). The genomic signature of parallel adaptation from shared genetic variation. Molecular Ecology *23*, 3944–3956.

14. Romundset, A., Lakeman, T.R., and Høgaas, F. (2018). Quantifying variable rates of postglacial relative sea level fall from a cluster of 24 isolation basins in southern Norway. Quaternary Science Reviews *197*, 175–192.

15. Sawyer, S., Krause, J., Guschanski, K., Savolainen, V., and Pääbo, S. (2012). Temporal Patterns of Nucleotide Misincorporations and DNA Fragmentation in Ancient DNA. PLOS ONE *7*, e34131.

16. Oosting, T., Star, B., Barrett, J.H., Wellenreuther, M., Ritchie, P.A., and Rawlence, N.J. (2019). Unlocking the potential of ancient fish DNA in the genomic era. Evolutionary Applications *12*, 1513–1522.

17. Skoglund, P., Ersmark, E., Palkopoulou, E., and Dalén, L. (2015). Ancient Wolf Genome Reveals an Early Divergence of Domestic Dog Ancestors and Admixture into High-Latitude Breeds. Current Biology *25*, 1515–1519.

18. Palkopoulou, E., Mallick, S., Skoglund, P., Enk, J., Rohland, N., Li, H., Omrak, A., Vartanyan, S., Poinar, H., Götherström, A., *et al.* (2015). Complete Genomes Reveal Signatures of Demographic and Genetic Declines in the Woolly Mammoth. Current Biology *25*, 1395–1400.

19. Ramos-Madrigal, J., Smith, B.D., Moreno-Mayar, J.V., Gopalakrishnan, S., Ross-Ibarra, J., Gilbert, M.T.P., and Wales, N. (2016). Genome Sequence of a 5,310-Year-Old Maize Cob Provides Insights into the Early Stages of Maize Domestication. Current Biology *26*, 3195–3201.

20. Noonan, J.P., Coop, G., Kudaravalli, S., Smith, D., Krause, J., Alessi, J., Chen, F., Platt, D., Paabo, S., Pritchard, J.K., *et al.* (2006). Sequencing and Analysis of Neanderthal Genomic DNA. Science *314*, 1113–1118.

21. McVean, G. (2009). A Genealogical Interpretation of Principal Components Analysis. PLoS Genet *5*, e1000686.

22. Charlesworth, B. (2009). Effective population size and patterns of molecular evolution and variation. Nat Rev Genet *10*, 195–205.

23. Li, H., and Durbin, R. (2011). Inference of human population history from individual whole-genome sequences. Nature *475*, 493–496.

24. Liu, S., Hansen, M.M., and Jacobsen, M.W. (2016). Region-wide and ecotype-specific differences in demographic histories of threespine stickleback populations, estimated from whole genome sequences. Mol. Ecol. *25*, 5187–5202.

25. Ceballos, F.C., Joshi, P.K., Clark, D.W., Ramsay, M., and Wilson, J.F. (2018). Runs of homozygosity: windows into population history and trait architecture. Nat Rev Genet *19*, 220–234.

26. Hermisson, J., and Pennings, P.S. (2017). Soft sweeps and beyond: understanding the patterns and probabilities of selection footprints under rapid adaptation. Methods in Ecology and Evolution *8*, 700–716.

27. Indjeian, V.B., Kingman, G.A., Jones, F.C., Guenther, C.A., Grimwood, J., Schmutz, J., Myers, R.M., and Kingsley, D.M. (2016). Evolving New Skeletal Traits by cis-Regulatory Changes in Bone Morphogenetic Proteins. Cell *164*, 45–56.

28. Peichel, C.L., Nereng, K.S., Ohgi, K.A., Cole, B.L.E., Colosimo, P.F., Buerkle, C.A., Schluter, D., and Kingsley, D.M. (2001). The genetic architecture of divergence between threespine stickleback species. Nature *414*, 901–905.

29. Colosimo, P.F., Peichel, C.L., Nereng, K., Blackman, B.K., Shapiro, M.D., Schluter, D., and Kingsley, D.M. (2004). The Genetic Architecture of Parallel Armor Plate Reduction in Threespine Sticklebacks. PLoS Biol *2*, e109.

30. Barrett, R.D.H., and Schluter, D. (2008). Adaptation from standing genetic variation. Trends in Ecology & Evolution *23*, 38–44.

31. Galloway, J., Cresko, W.A., and Ralph, P. (2019). A Few Stickleback Suffice for the Transport of Alleles to New Lakes. G3: Genes, Genomes, Genetics *10*, 505–514.

32. Fang, B., Kemppainen, P., Momigliano, P., Feng, X., and Merilä, J. (2020). On the causes of geographically heterogeneous parallel evolution in sticklebacks. Nat Ecol Evol.

33. DeFaveri, J., Shikano, T., Shimada, Y., Goto, A., and Merilä, J. (2011). Global analysis of genes involved in freshwater adaptation in threespine sticklebacks (Gasterosteus aculeatus). Evolution *65*, 1800–1807.

34. Liu, S., Ferchaud, A.-L., Grønkjær, P., Nygaard, R., and Hansen, M.M. (2018). Genomic parallelism and lack thereof in contrasting systems of three-spined sticklebacks. Molecular Ecology *27*, 4725–4743.

35. Terekhanova, N.V., Barmintseva, A.E., Kondrashov, A.S., Bazykin, G.A., and Mugue, N.S. (2019). Architecture of Parallel Adaptation in Ten Lacustrine Threespine Stickleback Populations from the White Sea Area. Genome Biology and Evolution *11*, 2605–2618.

36. Jowsey, P.C. (1966). An Improved Peat Sampler. New Phytologist *65*, 245–248.

37. Bennike, O. (1995). Palaeoecology of two lake basins from Disko, West Greenland. Journal of Quaternary Science *10*, 149–155.

38. Romundset, A., Fredin, O., and Høgaas, F. (2015). A Holocene sea-level curve and revised isobase map based on isolation basins from near the southern tip of Norway. Boreas *44*, 383–400.

39. Björck, S., Bennike, O., Ingólfsson, Ó., Barnekow, L., and Penney, D.N. (2008). Lake Boksehandsken's earliest postglacial sediments and their palaeoenvironmental implications, Jameson Land, East Greenland. Boreas *23*, 459–472.

40. Carøe, C., Gopalakrishnan, S., Vinner, L., Mak, S.S.T., Sinding, M.H.S., Samaniego, J.A., Wales, N., Sicheritz-Pontén, T., and Gilbert, M.T.P. (2018). Single-tube library preparation for degraded DNA. Methods in Ecology and Evolution *9*, 410–419.

41. Schubert, M., Lindgreen, S., & Orlando, L. (2016). AdapterRemoval v2: rapid adapter trimming, identification, and read merging. *BMC Research Notes*, *9*, 1-7.

42 Li, H., and Durbin, R. (2009). Fast and accurate short read alignment with Burrows-Wheeler transform. Bioinformatics *25*, 1754–1760.

43. Schubert, M., Ginolhac, A., Lindgreen, S., Thompson, J.F., AL-Rasheid, K.A., Willerslev, E., Krogh, A., and Orlando, L. (2012). Improving ancient DNA read mapping against modern reference genomes. BMC Genomics *13*, 178.

44. Li, H., Handsaker, B., Wysoker, A., Fennell, T., Ruan, J., Homer, N., Marth, G., Abecasis, G., and Durbin, R. (2009). The Sequence Alignment/Map format and SAMtools. Bioinformatics *25*, 2078–2079.

45. Smit, A., Hubley, R., and Green, P. (2015). RepeatMasker Open-4.0. <http://www.repeatmasker.org>.

46. Morgulis, A., Gertz, E.M., Schaffer, A.A., and Agarwala, R. (2006). WindowMasker: window-based masker for sequenced genomes. Bioinformatics *22*, 134–141.

47. Skoglund, P., Northoff, B.H., Shunkov, M.V., Derevianko, A.P., Pääbo, S., Krause, J., and Jakobsson, M. (2014). Separating endogenous ancient DNA from modern day contamination in a Siberian Neandertal. Proc Natl Acad Sci USA *111*, 2229–2234.

48. Dabney, J., Meyer, M., and Paabo, S. (2013). Ancient DNA Damage. Cold Spring Harbor Perspectives in Biology *5*, a012567–a012567.

49. Peyrégne, S., and Prüfer, K. Present-Day DNA Contamination in Ancient DNA Datasets. BioEssays, 2000081.

50. Fang, B., Merilä, J., Ribeiro, F., Alexandre, C.M., and Momigliano, P. (2018). Worldwide phylogeny of three-spined sticklebacks. Molecular Phylogenetics and Evolution *127*, 613–625.

51. Tracy, C.A., and Widom, H. (1994). Level-Spacing Distributions and the Airy Kernel. Commun.Math. Phys. *159*, 151–174.

52. Wang, L., Zhang, W., and Li, Q. (2020). AssocTests: An R Package for Genetic Association Studies. J. Stat. Soft. *94*.

53. Meisner, J., and Albrechtsen, A. (2018). Inferring Population Structure and Admixture Proportions in Low-Depth NGS Data. Genetics *210*, 719–731.

54. Skotte, L., Korneliussen, T.S., and Albrechtsen, A. (2013). Estimating Individual Admixture Proportions from Next Generation Sequencing Data. Genetics *195*, 693–702.

55. Evanno, G., Regnaut, S., and Goudet, J. (2005). Detecting the number of clusters of individuals using the software STRUCTURE: a simulation study. Mol. Ecol. *14*, 2611–2620.

56. Lawson, D.J., van Dorp, L., and Falush, D. (2018). A tutorial on how not to over-interpret STRUCTURE and ADMIXTURE bar plots. Nat Commun *9*, 3258.

57. Patterson, N., Price, A.L., and Reich, D. (2006). Population Structure and Eigenanalysis. PLoS Genet *2*, e190.

58. Janes, J.K., Miller, J.M., Dupuis, J.R., Malenfant, R.M., Gorrell, J.C., Cullingham, C.I., and Andrew, R.L. (2017). The K = 2 conundrum. Molecular Ecology *26*, 3594–3602.

59. Cullingham, C.I., Miller, J.M., Peery, R.M., Dupuis, J.R., Malenfant, R.M., Gorrell, J.C., and Janes, J.K. (2020). Confidently identifying the correct K value using the ΔK method: When does K = 2? Molecular Ecology *29*, 862–869.

60. Durand, E.Y., Patterson, N., Reich, D., and Slatkin, M. (2011). Testing for Ancient Admixture between Closely Related Populations. Molecular Biology and Evolution *28*, 2239–2252.

61. Korneliussen, T.S., Albrechtsen, A., and Nielsen, R. (2014). ANGSD: Analysis of Next Generation Sequencing Data. BMC Bioinformatics *15*, 356.

62. Guindon, S., and Gascuel, O. (2003). A Simple, Fast, and Accurate Algorithm to Estimate Large Phylogenies by Maximum Likelihood. Systematic Biology *52*, 696–704.

63. Mäkinen, H.S., and Merilä, J. (2008). Mitochondrial DNA phylogeography of the three-spined stickleback (Gasterosteus aculeatus) in Europe—Evidence for multiple glacial refugia. Molecular Phylogenetics and Evolution *46*, 167–182.

64. Feulner, P.G.D., Chain, F.J.J., Panchal, M., Huang, Y., Eizaguirre, C., Kalbe, M., Lenz, T.L., Samonte, I.E., Stoll, M., Bornberg-Bauer, E., *et al.* (2015). Genomics of Divergence along a Continuum of Parapatric Population Differentiation. PLoS Genet *11*, e1004966.

65. Purcell, S., Neale, B., Todd-Brown, K., Thomas, L., Ferreira, M.A.R., Bender, D., Maller, J., Sklar, P., de Bakker, P.I.W., Daly, M.J., *et al.* (2007). PLINK: A Tool Set for Whole-Genome Association and Population-Based Linkage Analyses. The American Journal of Human Genetics *81*, 559–575.

66. Ceballos, F.C., Hazelhurst, S., and Ramsay, M. (2018). Assessing runs of Homozygosity: a comparison of SNP Array and whole genome sequence low coverage data. BMC Genomics *19*, 106.

67. Danecek, P., Auton, A., Abecasis, G., Albers, C.A., Banks, E., DePristo, M.A., Handsaker, R.E., Lunter, G., Marth, G.T., Sherry, S.T., *et al.* (2011). The variant call format and VCFtools. Bioinformatics *27*, 2156–2158.

68. Li, H. (2011). A statistical framework for SNP calling, mutation discovery, association mapping and population genetical parameter estimation from sequencing data. Bioinformatics *27*, 2987–2993.

69. Weir, B.S., and Cockerham, C.C. (1984). Estimating F-Statistics for the Analysis of Population Structure. Evolution *38*, 1358–1370.

70. R Development Core Team (2010). R: a language and environment for statistical computing: reference index (R Foundation for Statistical Computing).

71. Hartl, D.L., and Clark, A.G. (2007). Principles of Population Genetics 4th ed. 2007. (Sinauer).

72. Friedman, J.H. (1984). A variable span scatterplot smoother. Laboratory for Computational Statistics, Stanford University Technical Report No. 5., 30.

73. Friedman, J.H. (1984). SMART user's guide (Laboratory for Computational Statistics, Dept. of Statistics, Stanford University).

74. Jónsson, H., Ginolhac, A., Schubert, M., Johnson, P.L.F., and Orlando, L. (2013). mapDamage2.0: fast approximate Bayesian estimates of ancient DNA damage parameters. Bioinformatics *29*, 1682–1684.

75. Haller, B.C., and Messer, P.W. (2019). SLiM 3: Forward Genetic Simulations Beyond the Wright–Fisher Model. Molecular Biology and Evolution *36*, 632–637.

KEY RESOURCES TABLE

KEY RESOURCES TABLE

REAGENT or RESOURCE	SOURCE	IDENTIFIER
Biological Samples		
Stickleback fin clip	This study	SAMN17375686
Stickleback fin clip	This study	SAMN17377651
Stickleback fin clip	This study	SAMN17377676
Stickleback fin clip	This study	SAMN17377678
Stickleback fin clip	This study	SAMN17377679
Stickleback fin clip	This study	SAMN17377782
Stickleback fin clip	This study	SAMN17377785
Stickleback fin clip	This study	SAMN17377787
Stickleback fin clip	This study	SAMN17377788
Stickleback fin clip	This study	SAMN17377789
Stickleback fin clip	This study	SAMN17377790
Stickleback fin clip	This study	SAMN17377791
Stickleback fin clip	This study	SAMN17377792
Stickleback fin clip	This study	SAMN17377793
Stickleback fin clip	This study	SAMN17377794
Stickleback fin clip	This study	SAMN17377795
Stickleback fin clip	This study	SAMN17377796
Stickleback fin clip	This study	SAMN17377797
Stickleback fin clip	This study	SAMN17377798
Stickleback fin clip	This study	SAMN17377799
Stickleback fin clip	This study	SAMN17377800
Stickleback fin clip	This study	SAMN17377804
Stickleback fin clip	This study	SAMN17377805
Stickleback fin clip	This study	SAMN17377806
Stickleback fin clip	This study	SAMN17377807
Stickleback fin clip	This study	SAMN17377886
Stickleback fin clip	This study	SAMN17377887
Stickleback fin clip	This study	SAMN17377888
Stickleback fin clip	This study	SAMN17377889
Stickleback fin clip	This study	SAMN17377898
Osteological remain	This study	SAMN17514713
Osteological remain	This study	SAMN17514712
Chemicals, Peptides, and Recombinant Proteins		
AmpliTaq Gold	Thermo Fisher Scientific	Cat# N8080241
N-Lauroylsarcosine solution 30% 500ml	Dutscher	Cat# 348533

Proteinase K 100MG	Thermo Fisher Scientific	Cat# 10103533
H2O, Molecular Biology Grade	Thermo Fisher Scientific	Cat# 10490025
Tween 20 100ML	Thermo Fisher Scientific	Cat# 10113103
Ethanol, Absolute, Mol Biology Grade	Thermo Fisher Scientific	Cat# 10644795
5M Sodium Chloride 100ML	Thermo Fisher Scientific	Cat# 10609823
guanidine hydrochloride	Sigma-Aldrich	Cat# G3272
2-Propanol	Merck	Cat# 109634
NEBNext End Repair Module	New England Biolabs	Cat# E6050L
Bst DNA Polymerase	New England Biolabs	Cat# M0275L
NEBNext Quick Ligation Module	New England Biolabs	Cat# E6056L
ACCUPRIME PFX DNA POLYMERASE 100mL	Thermo Fisher Scientific	Cat# 10472482
Agencourt AMPure XP - 60ml	Beckman Coulter	Cat# A63881
Buffer PE	QIAGEN	Cat# 19065
Buffer PB	QIAGEN	Cat# 19066
Buffer EB	QIAGEN	Cat# 19086
DMSO molecular biol 250ML	Thermo Fisher Scientific	Cat# 10397841
dNTP Set 100mM 100mL	Thermo Fisher Scientific	Cat# 10336653
EDTA 0.5M pH 8.0 Fisher Bioreagents 500ML	Thermo Fisher Scientific	Cat# 10182903
Tris HCl, 1M, pH 8.0, 100ML	Thermo Fisher Scientific	Cat# 10336763
Q5 High-Fidelity DNA Polymerase	New England Biolabs	Cat# M0491L
Critical Commercial Assays		
MinElute PCR Purification kit	QIAGEN	Cat# 28006
Tapestation screenTape D1000 HS	Agilent	Cat# 5067-5584
Qubit dsDNA HS Assay Kit	Thermo Fisher Scientific	Cat# Q32854
Deposited Data		
Raw sequence data (fastq format)	This study	NCBI: PRJNA693136
Software and Algorithms		
AdapterRemoval v2	41	https://github.com/MikkelSchubert/adapterremoval
ANGSD	61	http://www.popgen.dk/angsd/index.php/ANGSD
AssocTests	52	https://cran.r-project.org/web/packages/AssocTests/index.html
bcftools	67	http://samtools.github.io/bcftools/bcftools.html
BWA	42	https://github.com/lh3/bwa
mapDamage	74	https://ginolhac.github.io/mapDamage/
NGSadmix	54	http://www.popgen.dk/software/index.php/NgsAdmixv2

PCAngsd	53	https://github.com/Rosemeis/pcangsd
PhyML	62	https://github.com/stephaneguindon/phyml
PLINK	65	http://zzz.bwh.harvard.edu/plink/
PMDtools	47	https://github.com/pontussk/PMDtools
PSMC	23	https://github.com/lh3/psmc
RepeatMasker	45	http://www.repeatmasker.org
Samtools	44	http://www.htslib.org
SLiM 3.0	75	https://messerlab.org/slim/
VCFtools	67	https://vcftools.github.io/man_latest.html
WindowMasker	46	https://github.com/goeckslab/WindowMasker

Figure 1

A

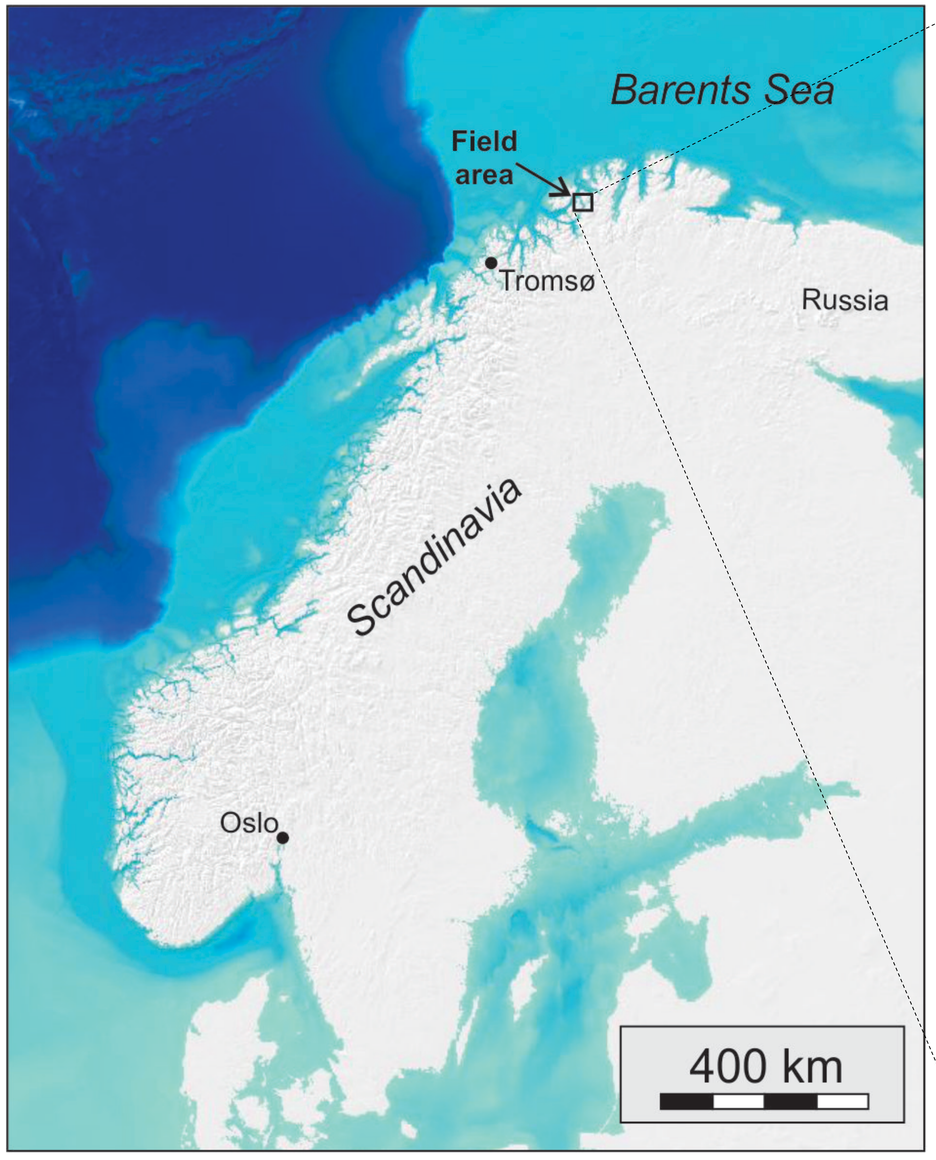
Barents Sea
Field area
Tromsø
Russia
Scandinavia
Oslo
400 km

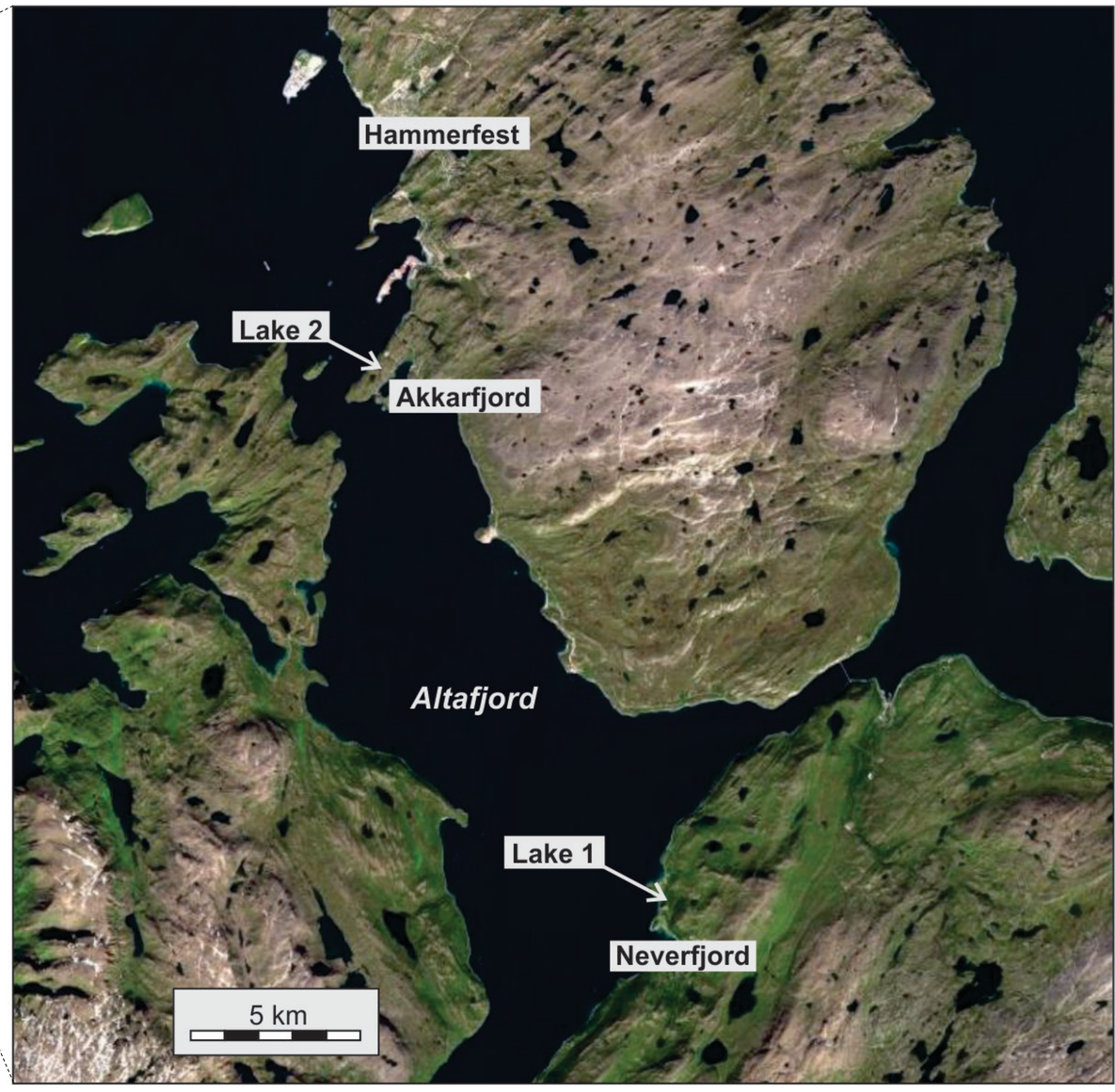
Hammerfest
Lake 2
Akkarfjord
Altafjord
Lake 1
Neverfjord
5 km

B

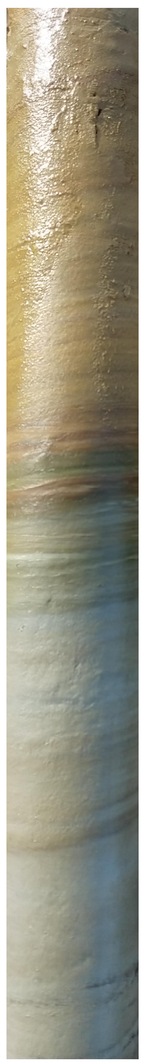

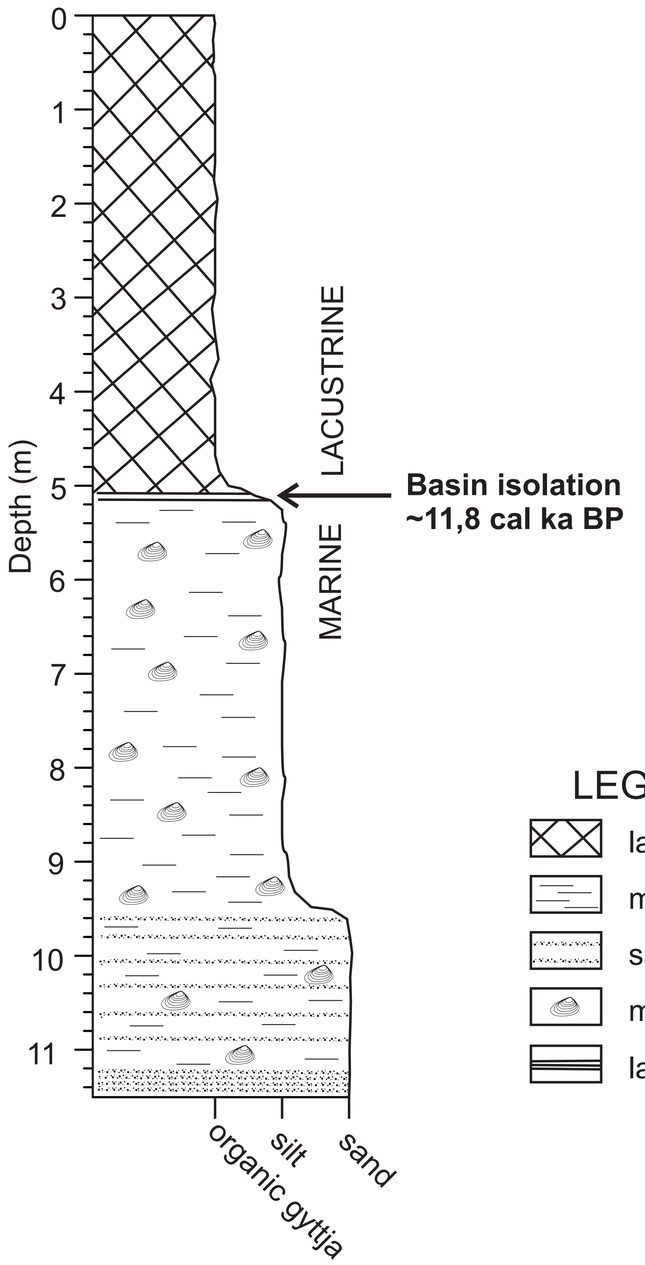
Lake 1: Klubbvatnet, Neverfjord, 33.2 m asl.
Depth (m)
0
1
2
3
4
5
6
7
8
9
10
11
LACUSTRINE
MARINE
Basin isolation ~11,8 cal ka BP
organic gyttja
silt
sand

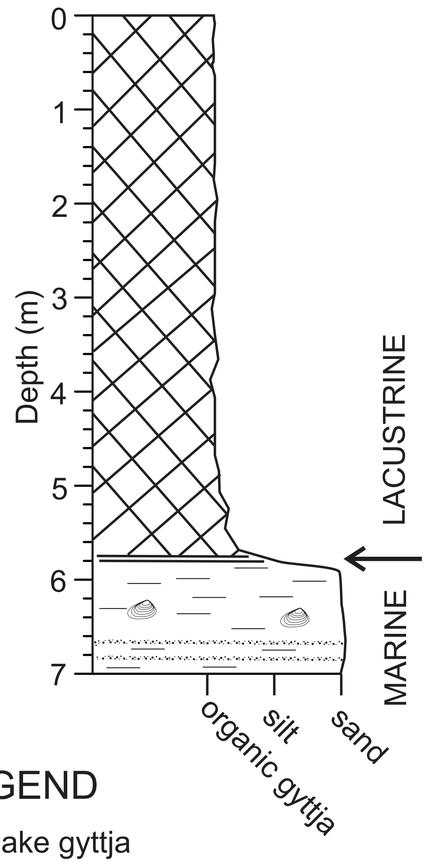
Lake 2: Jossavannet, Akkarfjord, 38.4 m asl.
Depth (m)
0
1
2
3
4
5
6
7
LACUSTRINE
MARINE
Basin isolation ~12,9 cal ka BP
organic gyttja
silt
sand

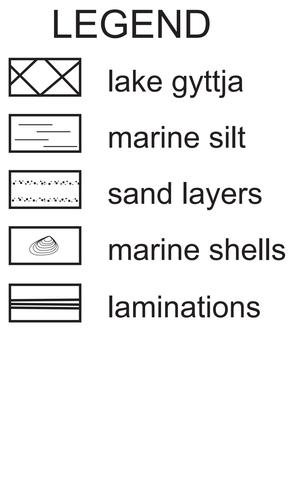
LEGEND
lake gyttja
marine silt
sand layers
marine shells
laminations

C

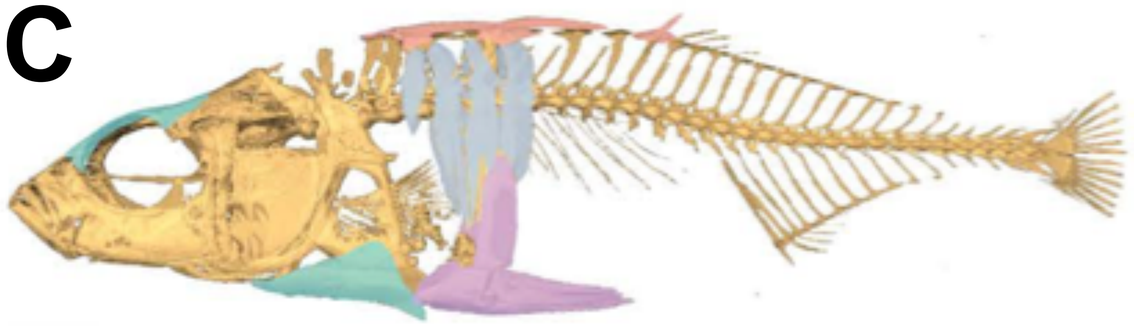

Figure 2

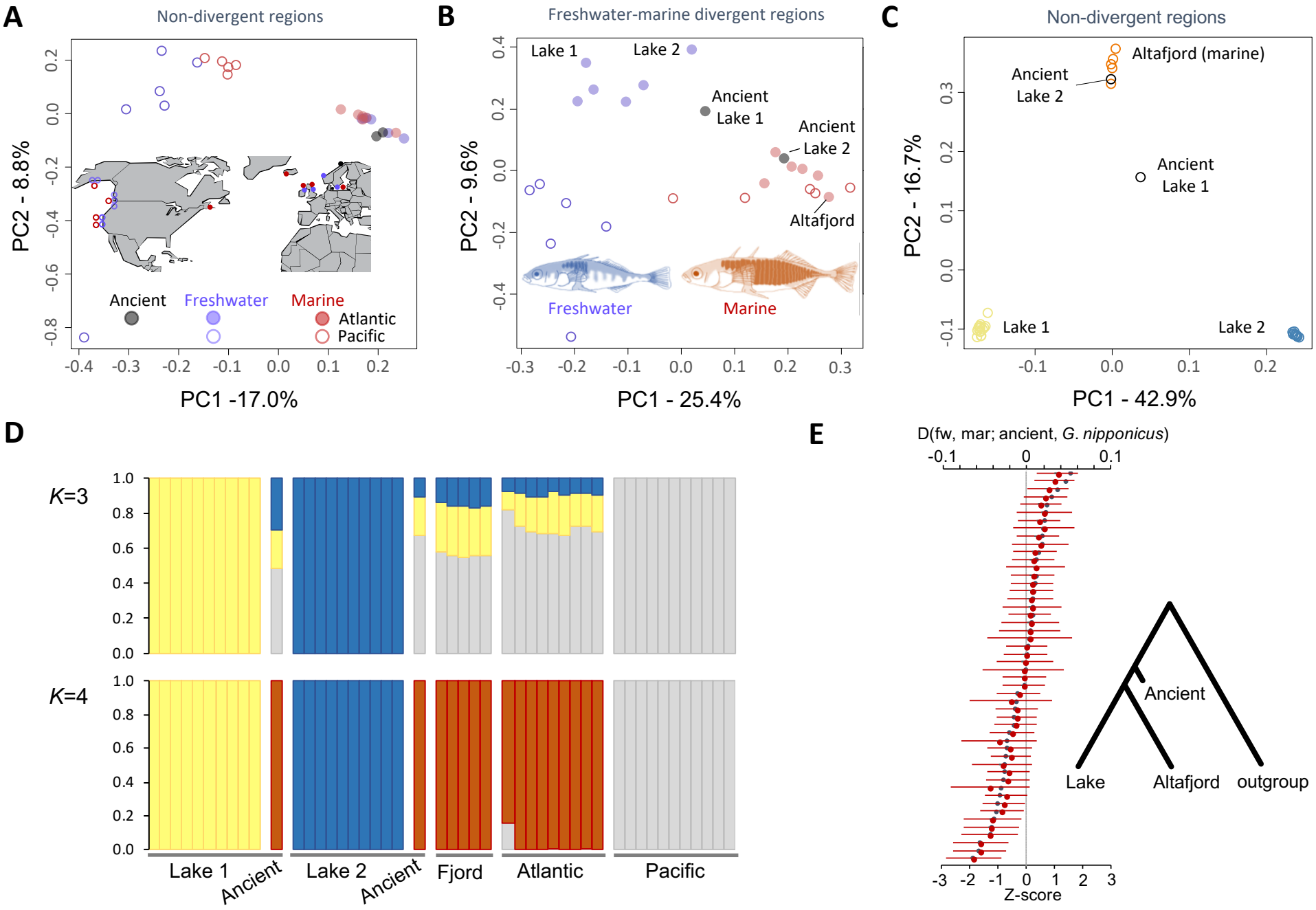
A
Non-divergent regions
PC2 - 8.8%
PC1 -17.0%
Ancient
Freshwater
Marine
Atlantic
Pacific
B
Freshwater-marine divergent regions
Lake 1
Lake 2
Ancient Lake 1
Ancient Lake 2
Altafjord
Freshwater
Marine
PC2 - 9.6%
PC1 - 25.4%
C
Non-divergent regions
Altafjord (marine)
Ancient Lake 2
Ancient Lake 1
Lake 1
Lake 2
PC2 - 16.7%
PC1 - 42.9%
D
K=3
K=4
Lake 1
Ancient
Lake 2
Ancient
Fjord
Atlantic
Pacific
E
D(fw, mar; ancient, G. nipponicus)
Z-score
Ancient
Lake
Altafjord
outgroup

Figure 3

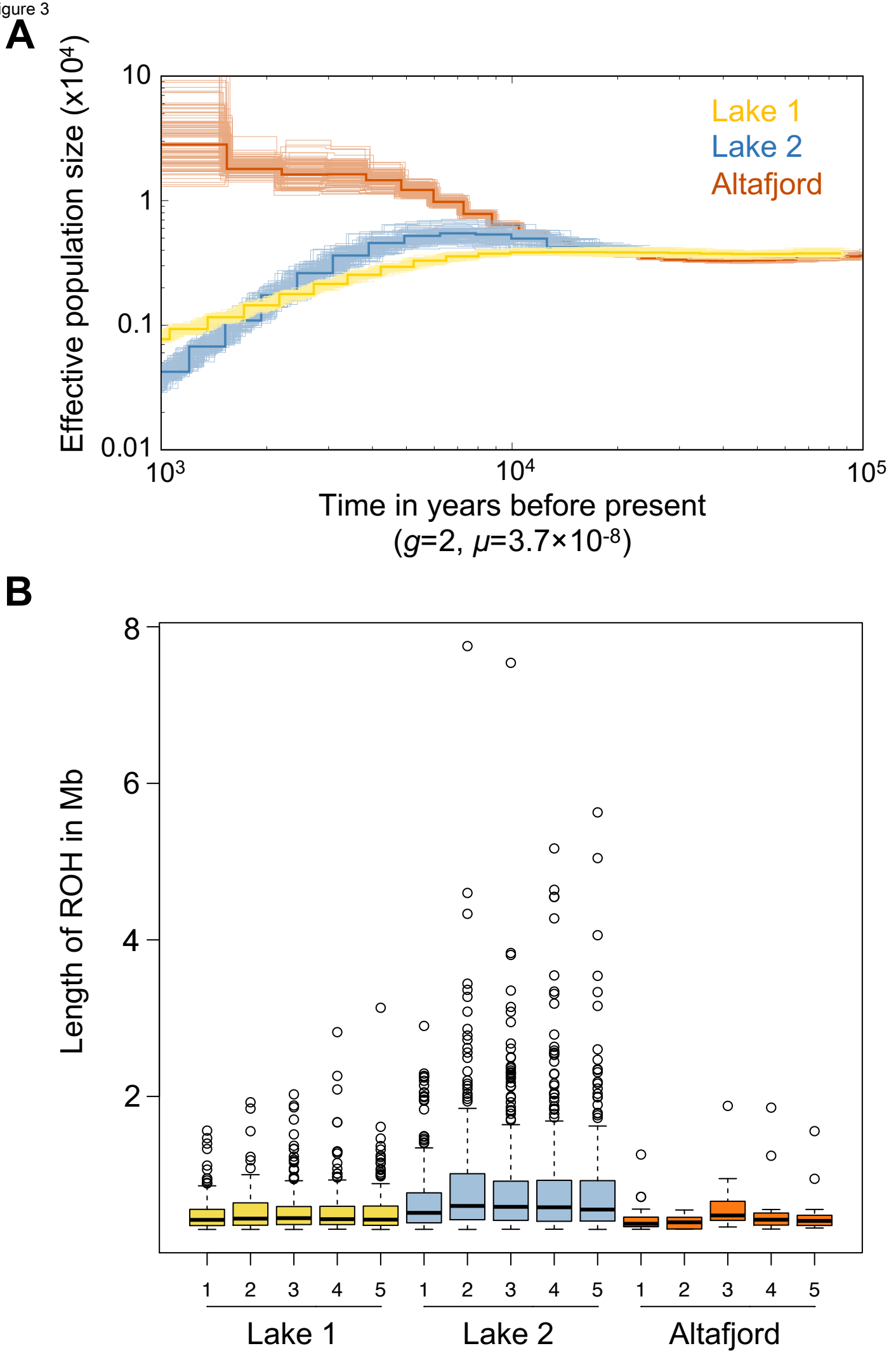
A
Effective population size (x10⁴)
10
1
0.1
0.01
10³
10⁴
10⁵
Lake 1
Lake 2
Altafjord
Time in years before present
(g=2, μ=3.7×10⁻⁸)
B
Length of ROH in Mb
8
6
4
2
1 2 3 4 5 1 2 3 4 5 1 2 3 4 5
Lake 1
Lake 2
Altafjord

Figure 4

A

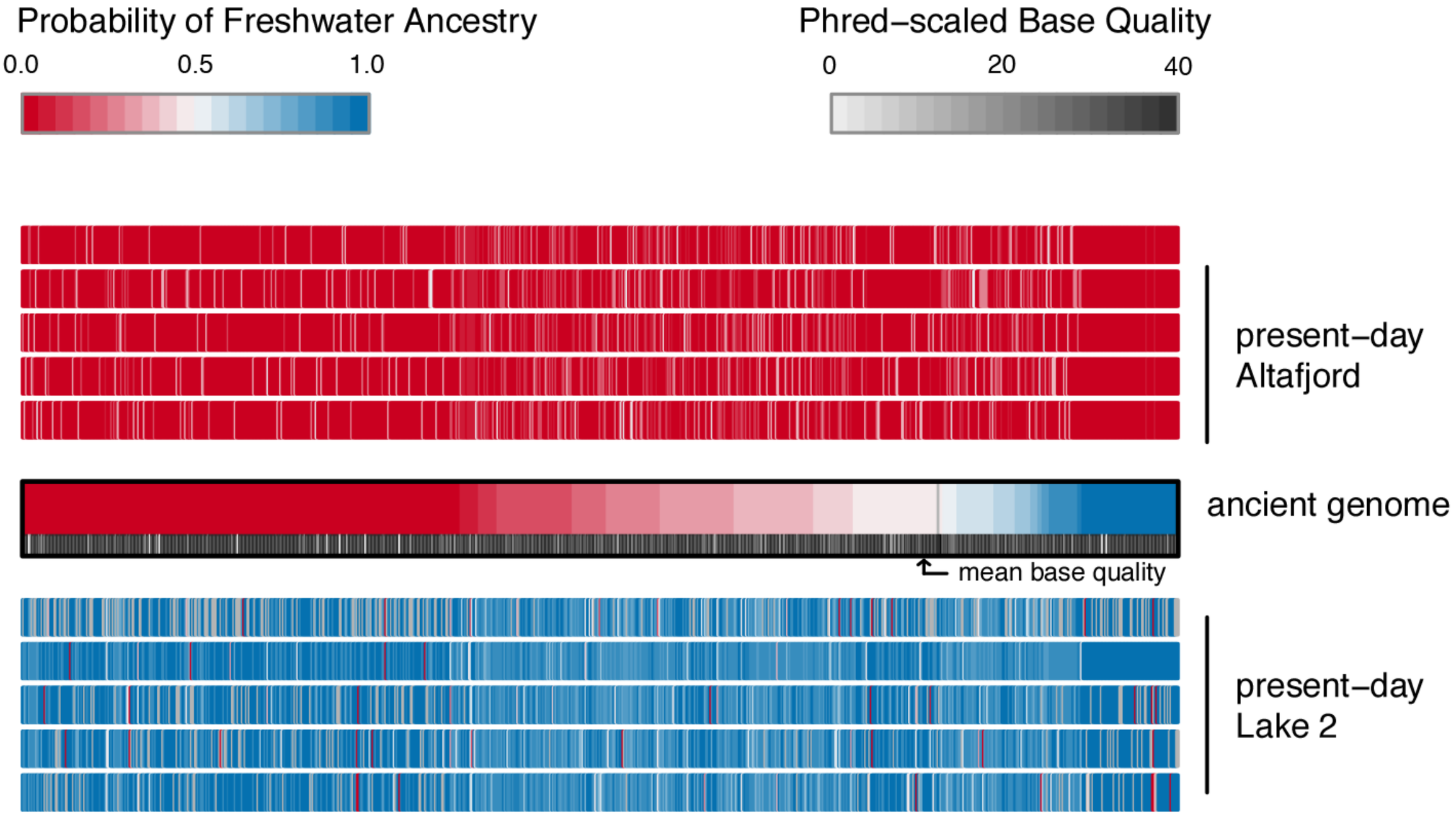
Probability of Freshwater Ancestry
0.0
0.5
1.0
Phred−scaled Base Quality
0
20
40
present−day
Altafjord
ancient genome
mean base quality
present−day
Lake 2

B

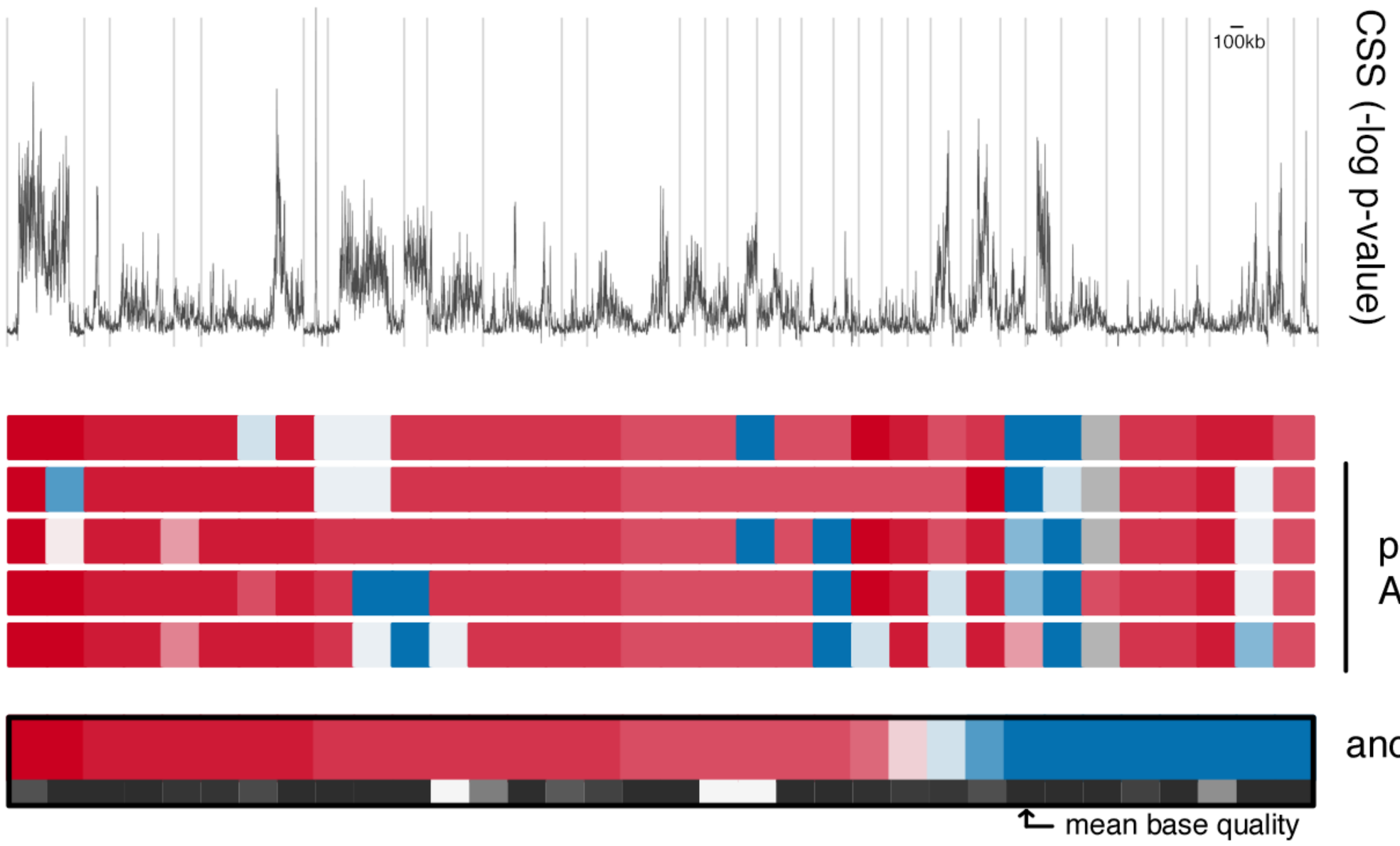
100kb
CSS (-log p-value)
present−day
Altafjord
ancient genome
mean base quality
present−day
Lake 2

C

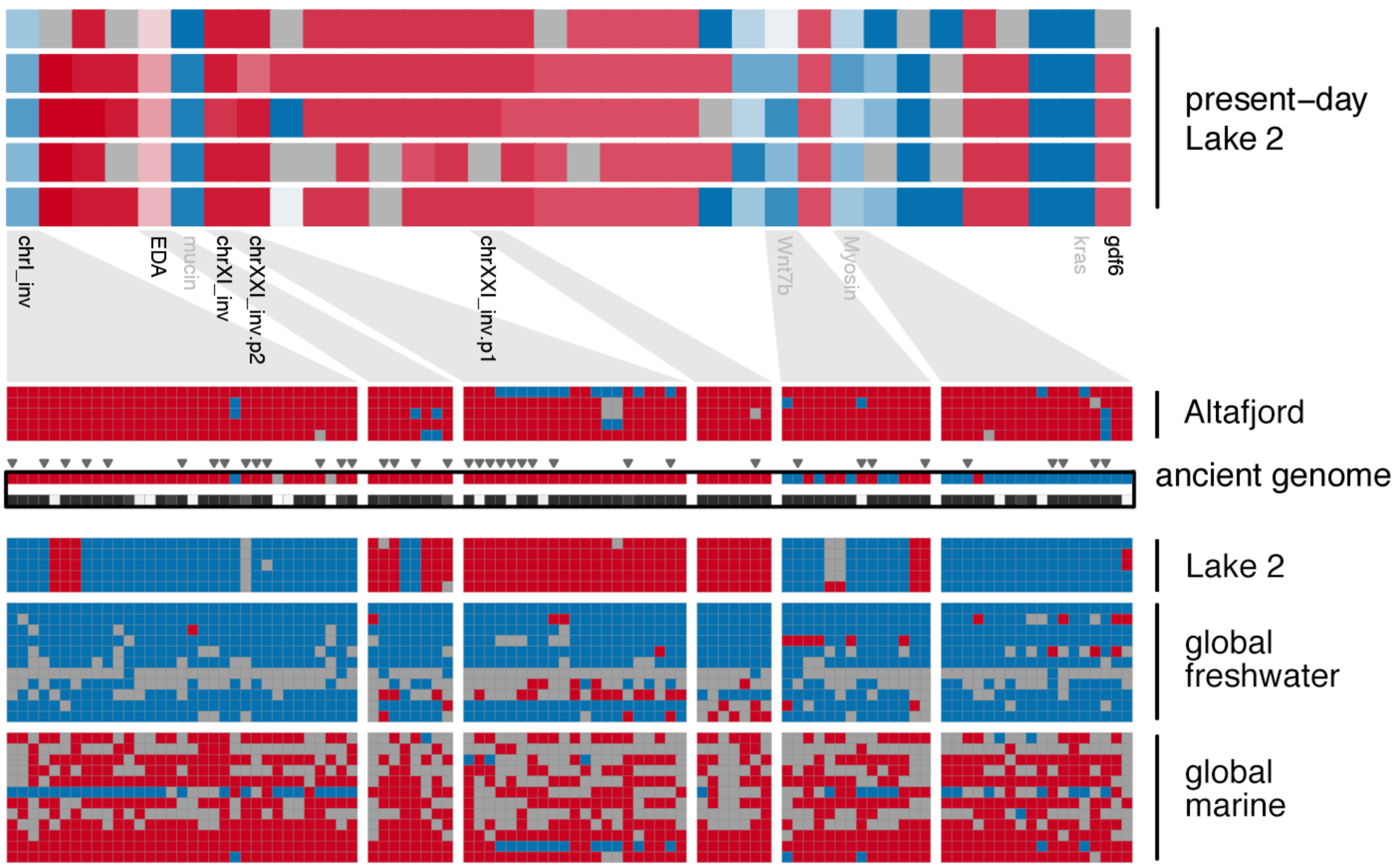
chrI_inv
EDA
mucin
chrXI_inv
chrXXI_inv.p2
chrXXI_inv.p1
Wnt7b
Myosin
kras
gdf6
Altafjord
ancient genome
Lake 2
global
freshwater
global
marine

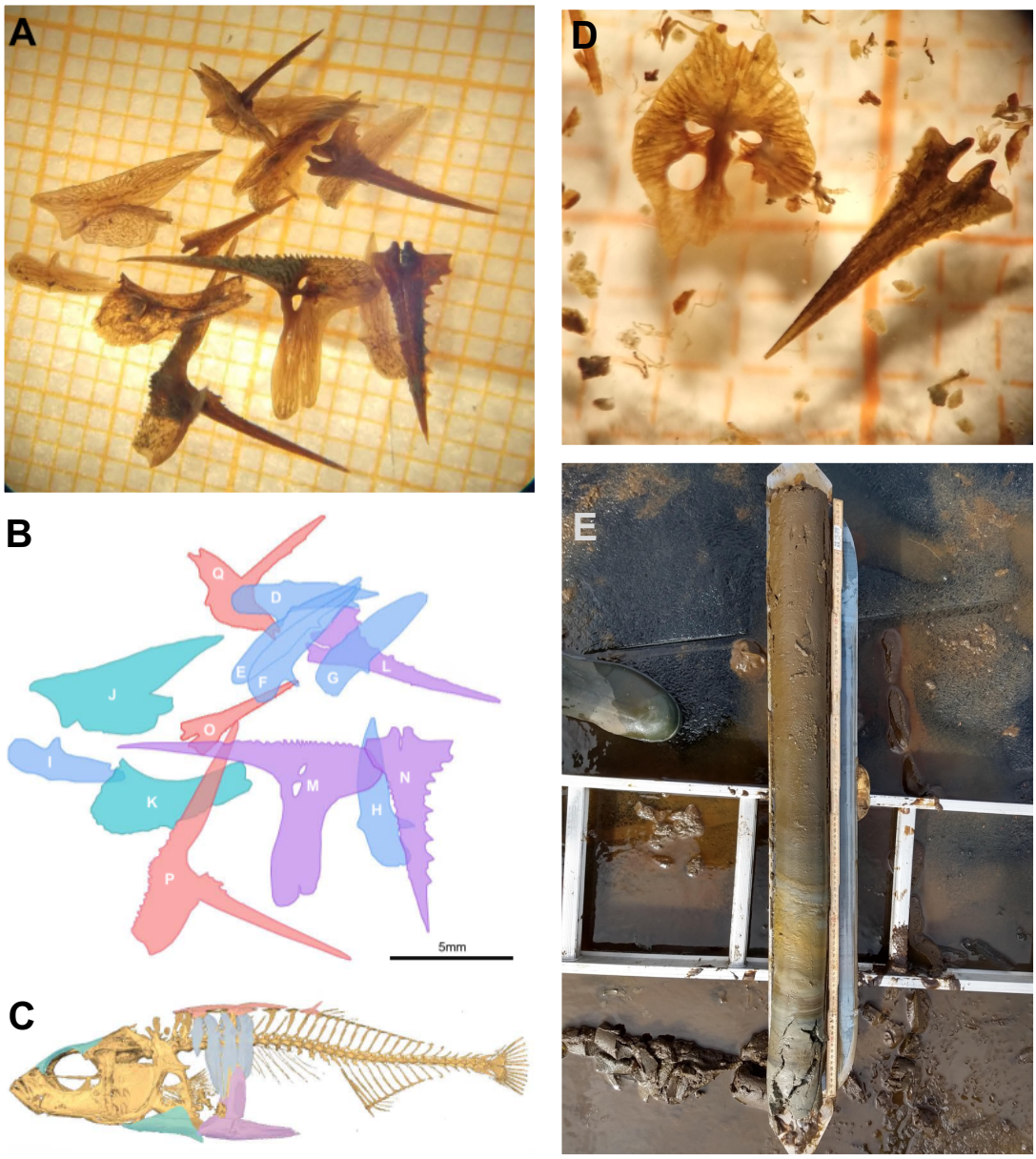

Figure S1. Ancient stickleback bones, plates and spines. (A) Photograph of bones from Lake 1 (Klubbvatnet) near Neverfjord, Finnmark, Norway. Small squares on the backing paper are 2mm^2. (B) Illustration of bone identities from (A). D-I (blue) are lateral plates. J and K (turquoise) are from the head area. J is the plate-like dermal bone between the gills and the pelvis (ectocoracoid). K is the part of the skull plate that is above the eye (frontal). L, M and N (violet) are the pelvic bones: L and N are the pelvic spines, M is the spine-like element between them and part of the lateral protrusion. O, P and Q (red) are dorsal spines; O has lost its basal plate, while P and Q retain theirs. Scale bar in lower right corner is 5mm. (C) Positions of bones from (A & B) illustrated on an X-Ray scan of a modern freshwater fish. (D) Photograph of bones from Lake 2 (Jossavannet) near Hammerfest, Finnmark, Norway. Small squares on the backing paper are 2mm^2. (E) Sediment core from Lake 2. The marine phase of the core is on the right-side of the photograph, which is characterized by marine clay, silt and sand, which transitions to clay gyjttja with laminations during the phase where the lake is partially isolated with occasional marine contact, and then to freshwater gyttja as the lake became fully isolated.

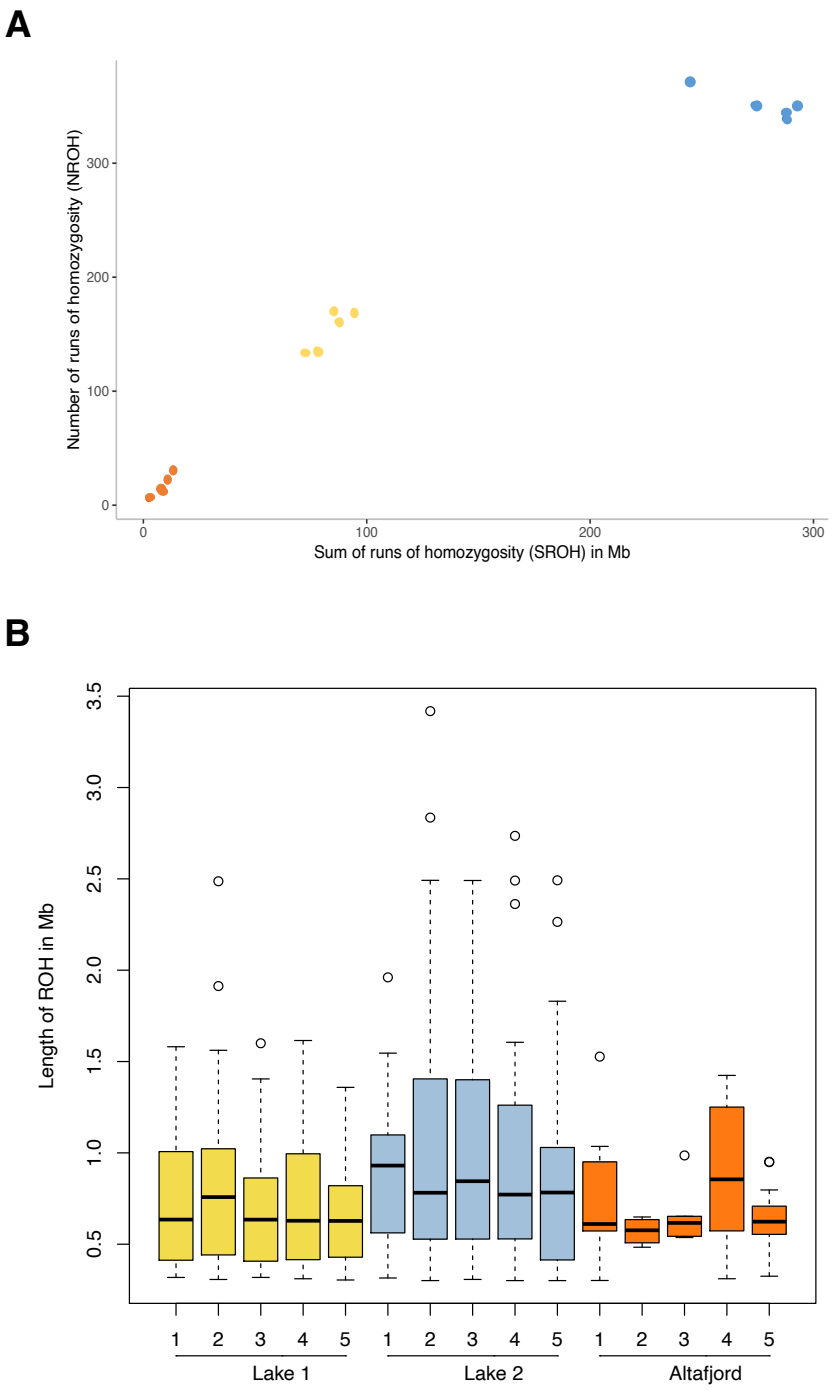

Figure S2. **Runs of homozygosity (ROH) estimates** (A) The sum and number of ROH for the five highest coverage genomes from Lake 1 (yellow), Lake 2 (blue) and Altafjord (orange). (B) Distribution of the length of ROH greater than 0.3 Mb in the 242 regions of the genome associated with marine-freshwater divergence in five genomes each from Lake 1 (yellow), Lake 2 (blue) and Altafjord (orange). The thick black line shows the median. The bottom and top of the box represent the 1st (Q1) and 3rd (Q3) quartile. The upper whisker corresponds to the smaller value of the maximum length of ROH or the sum of Q3 and 1.5 times the size of the box (Q3-Q1). All values above the upper whisker are shown as black circles. The lower whisker shows the smallest length of ROH for the corresponding individual.

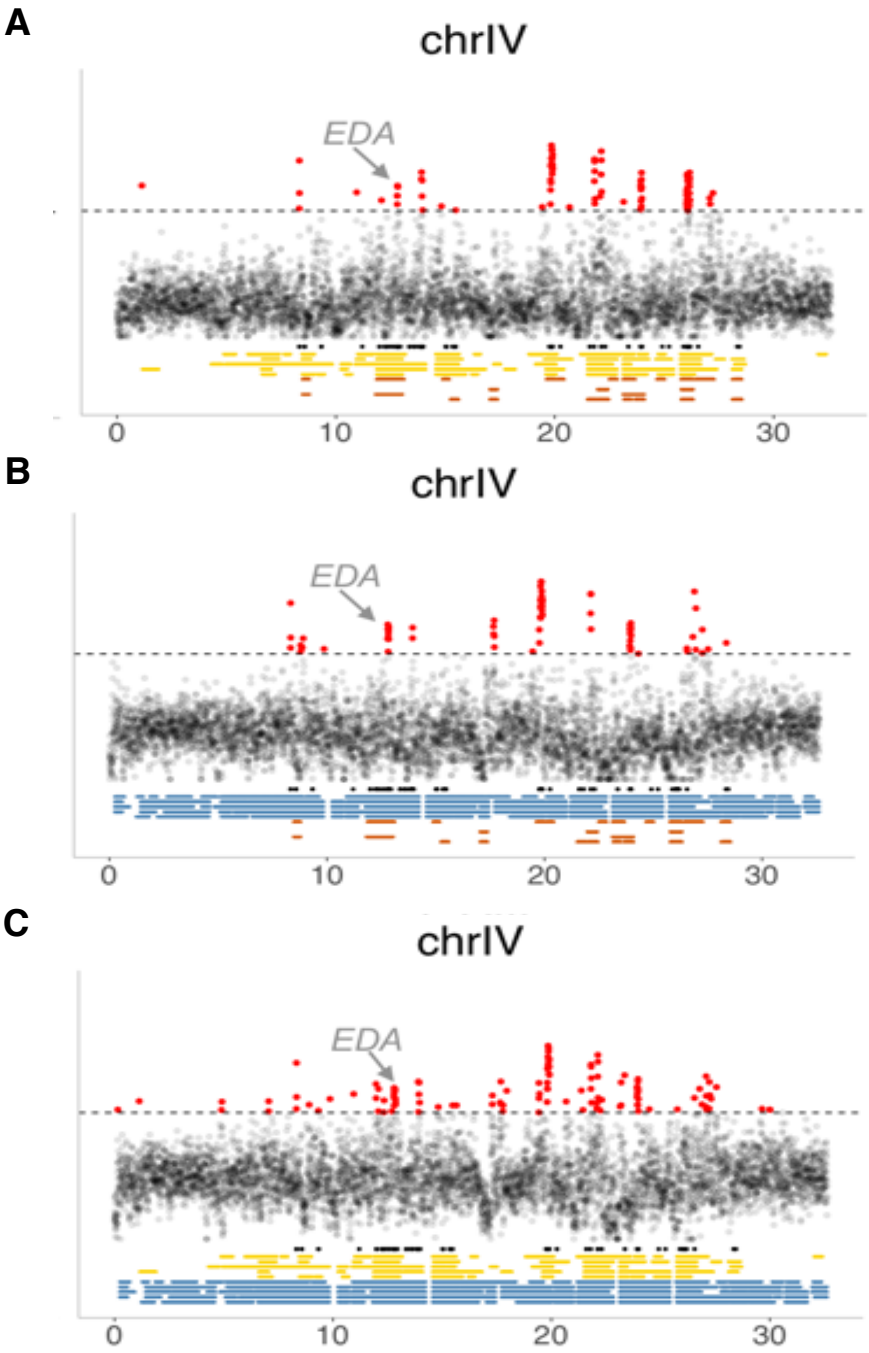

Figure S3. Manhattan plots of F_{ST} estimates for chromosome IV between (A) Lake 1 and Altafjord, (B) Lake 2 and Altafjord, and (C) Lake 1 and Lake 2. Manhattan plots of F_{ST} values (*y*-axis) estimated for 10kb sliding windows at sliding intervals of 5 kb. The steps on the x-axis represent Mb along the chromosome. Values above F_{ST} = 0.5 are coloured red and a dotted marker line is inserted at F_{ST} = 0.5. The black bars underneath the Manhattan plot show the location of the divergent regions from Jones *et al.*[S1] (FDR 0.05), whereas yellow, blue and orange bars represent the locations of the ROHs > 0.3 Mb of five individuals from Lake 1, Lake 2 and Altafjord, respectively.

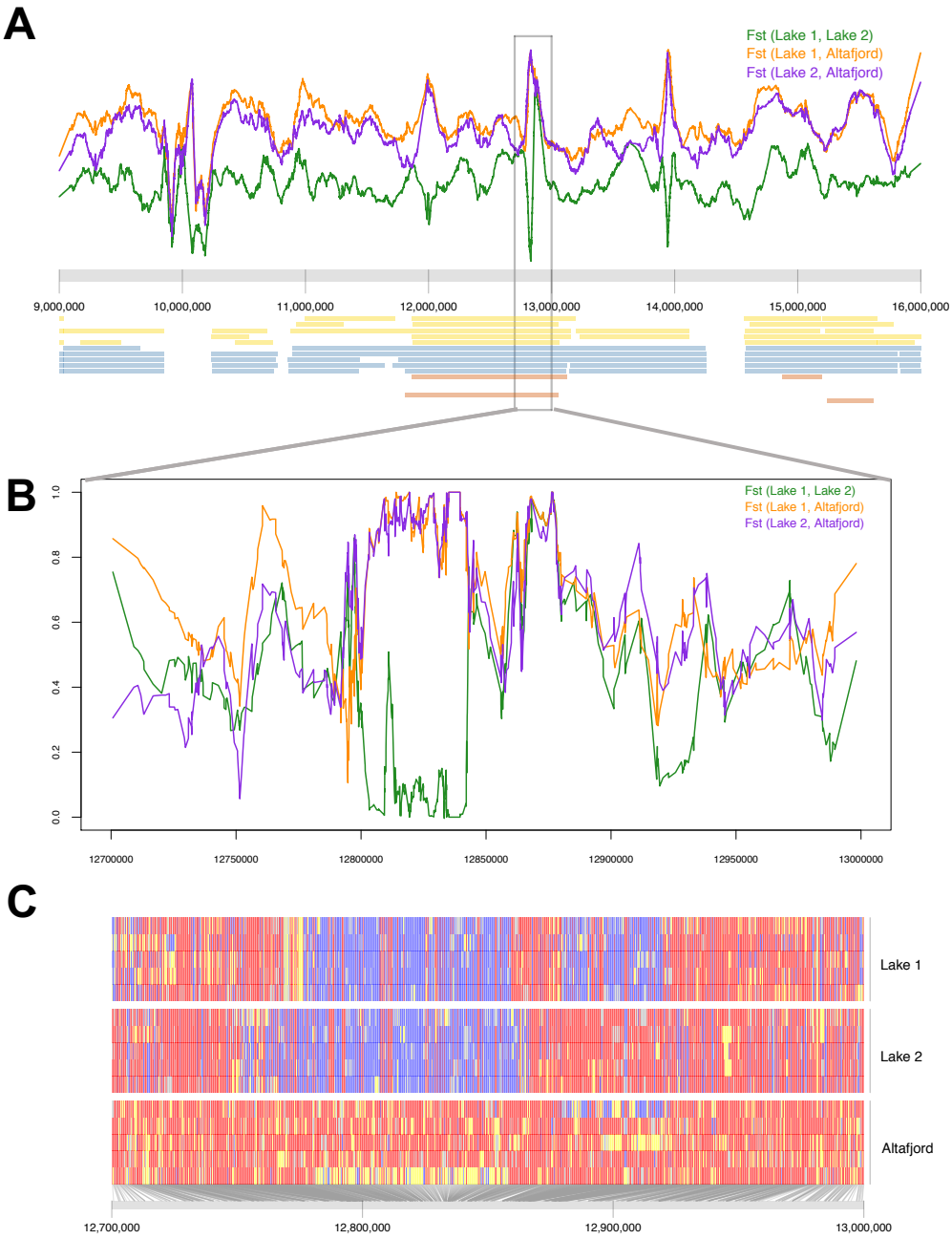

Figure S4. Freshwater populations carry different EDA haplotype.
(A) F_{ST} analyses and ROH for Lake 1, Lake 2 and Altafjord on chrIV:9,000,000-16,000,000 around the EDA region. The upper part shows curves for the F_{ST} values between each two populations, whereas the yellow, blue and red bars underneath the plot represent the locations of the ROHs > 0.3 Mb of five individuals from Lake 1, Lake 2 and Altafjord, respectively. (B) F_{ST} analyses for Lake 1, Lake 2 and Altafjord on chrIV:12,700,000-13,000,000 around the focal EDA region. The curves show F_{ST} values between each two populations. (C) Underlying genotypes at 1200 randomly picked single nucleotide polymorphisms within chrIV:12,700,000-13,000,000. Rows represent individual fish; columns represent individual single nucleotide polymorphisms; red boxes indicate alleles most common in the marine population; blue boxes indicate alleles less common in the marine population; grey boxes are missing data.

Sample Name	Location
ABW_19_Fresh	River Tyne, Scotland
ANTL_07_Marine	Antigonish Landing, Nova Scotia, Canada
BDGB_04_Marine	Bodega Bay, CA, USA
BIGL_12_Fresh	Big River Lagoon, CA, USA
BIGR_05_Marine	Big River, CA, USA
FTC_14_Fresh	Fish Trap Creek, WA, USA
GJOG_06_Marine	Gjögur, Iceland
GORT_08_Marine	Gorten Sands, Scotland
HUTU_13_Fresh	Humptulips, WA, USA
JAMA_10_Marine	Japan Marine
JMRP_09_Marine	River Tyne, Scotland
MATA_11_Fresh	Matadero Creek, CA, USA
MUDL_15_Fresh	Mud Lake, AK, USA
Neu_Marine	Neustadt, Germany
NOST_Stream	Stream, Norway
PAXB_20_Fresh	Paxton Lake, B.C. Canada
RABS_01_Marine	Rabbit Slough, AK, USA
SALR_02_MAR	Salmon River, B.C. Canada
SCX_17_Fresh	Schwalle River, Germany
SHEL_18_Fresh	River Shiel, Scotland
Lake 1	Klubbvatnet Lake, Finnmark, Norway
Lake 2	Jossavannet Lake, Finnmark, Norway
Altafjord	Altafjord, Finnmark, Norway

Table S1. The global dataset used in two PCAs and admixture analysis consists of twenty samples from Jones *et al.*[S1] and one sample each from Lake 1, Lake 2 and Altafjord.

Sample Name	Location	Coverage (sequenced)	Accession
Ancient_01	Lake 1	<1x	SAMN17514712
Ancient_02	Lake 2	<1x	SAMN17514713
Fish_01	Lake 1	2.88	SRR13517313
Fish_02	Lake 1	9.35	SRR13517312
Fish_03	Lake 1	3.03	SRR13517301
Fish_04	Lake 1	11.42	SRR13517290
Fish_05	Lake 1	13.57	SRR13517289
Fish_06	Lake 1	3.31	SRR13517288
Fish_07	Lake 1	4.67	SRR13517287
Fish_08	Lake 1	3.64	SRR13517286
Fish_09	Lake 1	2.91	SRR13517285
Fish_10	Lake 1	2.81	SRR13517284
Fish_11	Lake 1	11.64	SRR13517311
Fish_12	Lake 1	9.67	SRR13517310
Fish_13	Lake 1	2.89	SRR13517309
Fish_14	Lake 1	3.04	SRR13517308
Fish_15	Lake 1	3.54	SRR13517307
Fish_16	Lake 2	7.53	SRR13517306
Fish_17	Lake 2	3.01	SRR13517305
Fish_18	Lake 2	10.56	SRR13517304
Fish_19	Lake 2	2.66	SRR13517303
Fish_20	Lake 2	10.10	SRR13517302
Fish_21	Lake 2	2.16	SRR13517300
Fish_22	Lake 2	2.80	SRR13517299
Fish_23	Lake 2	11.45	SRR13517298
Fish_24	Lake 2	5.97	SRR13517297
Fish_25	Lake 2	16.75	SRR13517296
Fish_26	Altafjord	7.82	SRR13517295
Fish_27	Altafjord	14.70	SRR13517294
Fish_28	Altafjord	11.56	SRR13517293
Fish_29	Altafjord	12.05	SRR13517292
Fish_30	Altafjord	9.02	SRR13517291

Table S2. Mean depth of coverage per genome for each of the local modern stickleback samples sequenced for this study referred to as ‘local’ population dataset.

Supplemental References

S1. Jones, F.C., Grabherr, M.G., Chan, Y.F., Russell, P., Mauceli, E., Johnson, J., Swofford, R., Pirun, M., Zody, M.C., White, S., *et al.* (2012). The genomic basis of adaptive evolution in threespine sticklebacks. Nature *484*, 55–61.

Methods S1

Further methodological details and results, and simulations to validate empirical results. Related to STAR Methods, Figures 2, 3 and S3.

1 Postmortem damage patterns

DNA can survive millennia post-mortem, spanning ecological and evolutionary transitions and providing a unique window into the processes underlying biodiversity. As such sequencing ancient DNA from temporally spaced samples can allow the testing of hypotheses related to evolutionary responses to ecological change and novel selection pressures through direct quantification of ecological and genetic parameters collected before, during and after genetic changes in selection pressures. However, post-mortem deamination of cytosine to uracil, which is read as thymine by the sequencer, produces characteristic DNA damage patterns of an excess of cytosine to thymine at the 5′ termini, and the reverse complement at the 3′ termini. These post-mortem damage patterns require consideration in downstream analyses, for example by excluding transversions or recalibration of base quality scores based on read position. DNA damage patterns are also a useful authentication of a samples age.

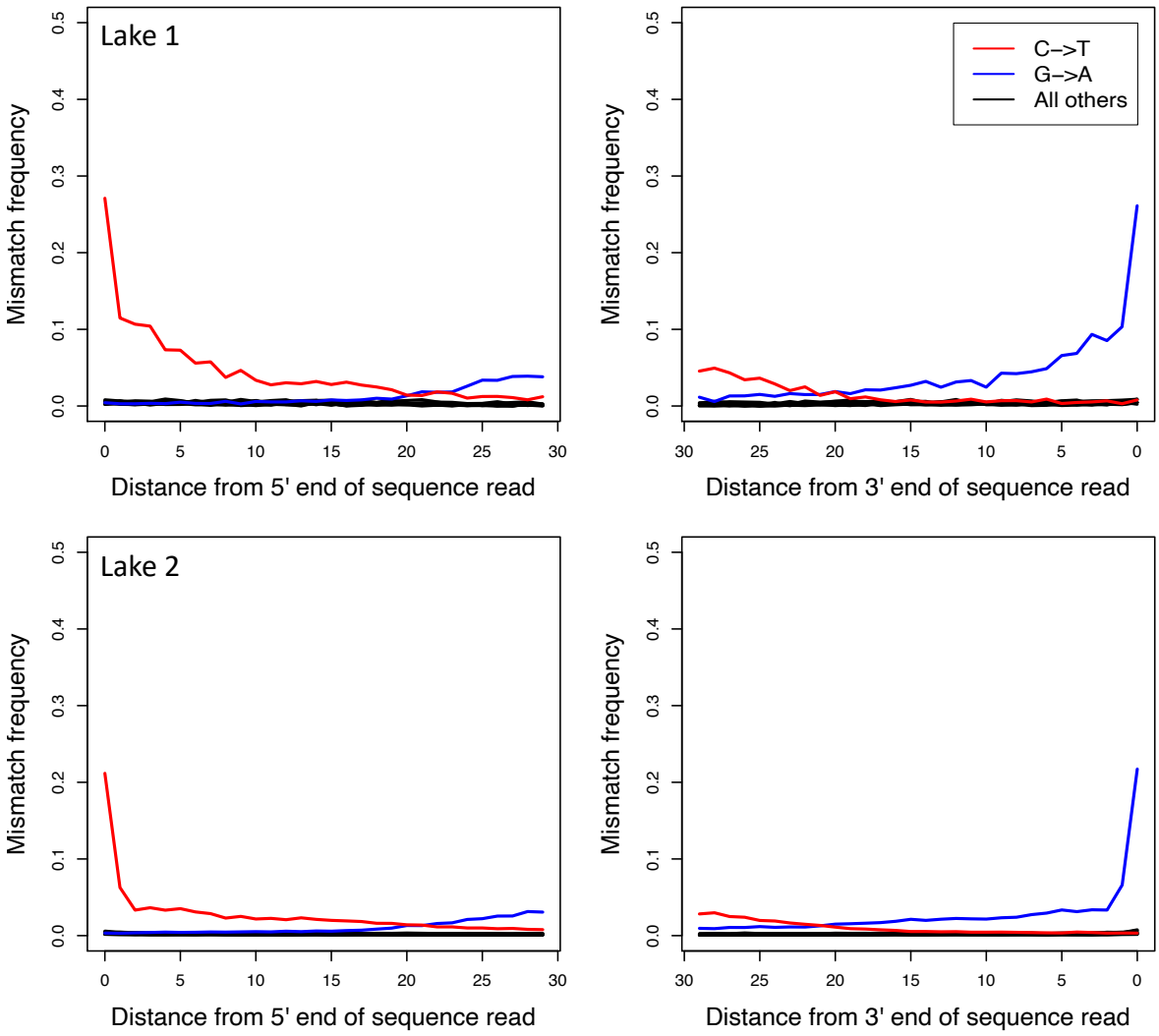

DNA misincorporation errors at the 5′ and 3′ read termini sequence data generated from DNA extracted from the ancient samples from Lake 1 and Lake 2 showed the characteristic (C>T and G>A) post-mortem damage patterns relative to the modern stickleback reference (gasAcu1).

2 Principal Component Analysis

We conducted Principal Component Analysis (PCA) on four datasets. The first two PCA were performed on the global dataset, first excluding regions that were found to show global divergence between marine and freshwater stickleback by Jones *et al.*[S1], and second only considering the marine-freshwater divergent regions (Figure 2A-B). These two comparisons highlight how the non-divergent regions show a pattern whereby genes mirror geography; whereas the marine-freshwater divergent regions show a pattern of variation in which genes mirror ecology. The eigen vectors 1-10 are shown below.

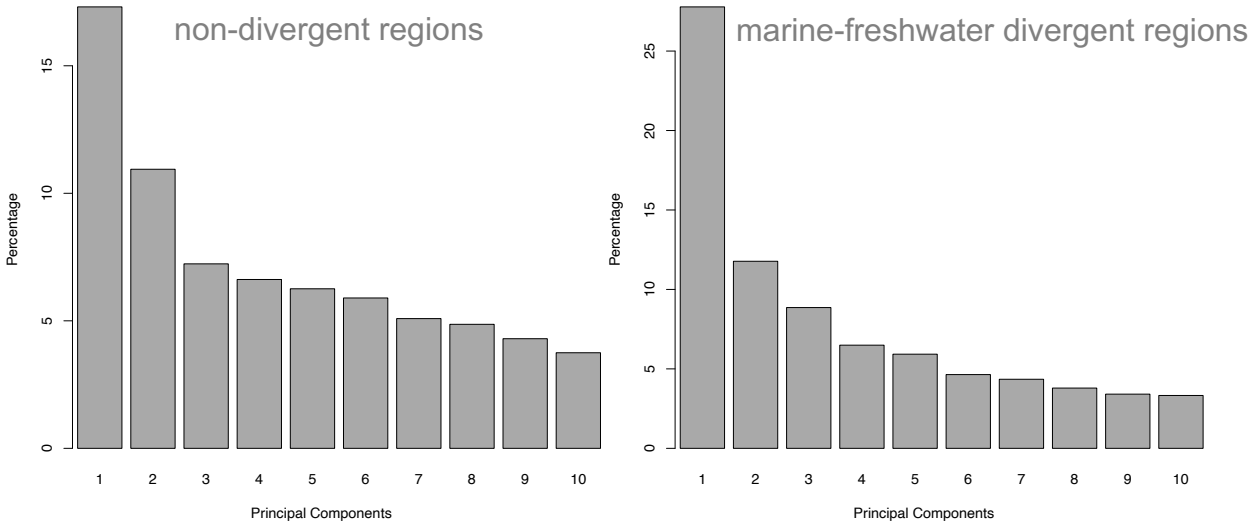

We then performed PCA on the focal study populations (*i.e.* Lake 1, Lake 2 and Altafjord), again considering first the non-divergent regions (Figure 2C) and then the marine-freshwater divergent regions. The eigen vectors 1-10 are shown below, with the PCA plot for PCs 1 and 2 for marine-divergent regions embedded.

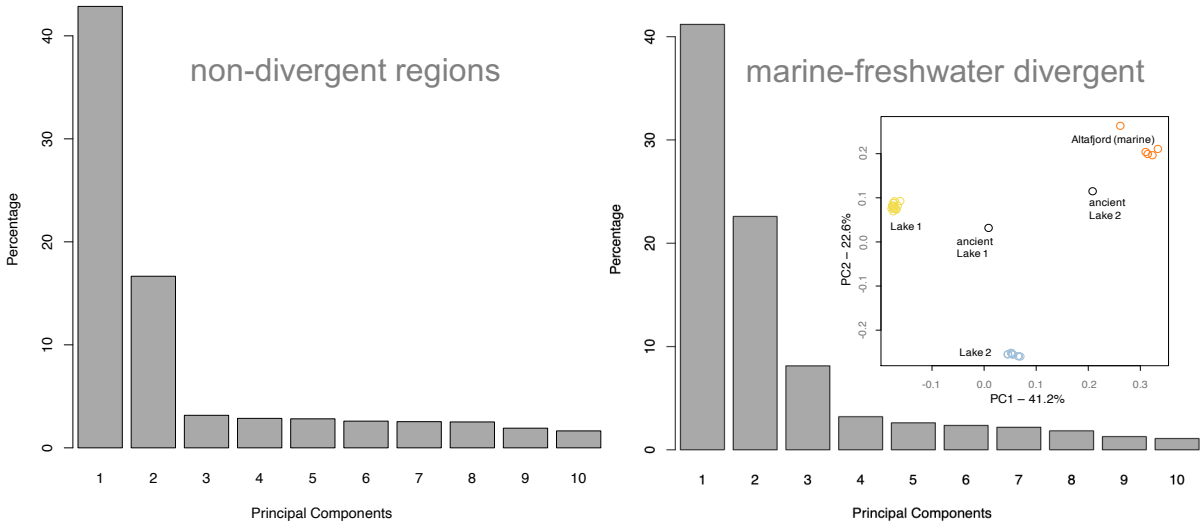

3 Pairwise Sequentially Markovian Coalescent

Bias can be introduced into the PSMC estimates of effective populations size through time when comparing sequences of low and differing coverage, which results in different rates of false negative detection of heterozygote sites, producing the same effect as using a lower mutation rate for the sequence with lower coverage. In order to better understand if sequencing coverage impacted our inference of demographic histories and the underlying processes, PSMC was used to analyse down-sampled versions of the high coverage freshwater stickleback genome (sample BS65 from Feulner *et al.*[S2]). We found that lower coverage genomes underestimated ancestral effective population size, but the overall trajectory of the plot of effective population size through time remained consistent:

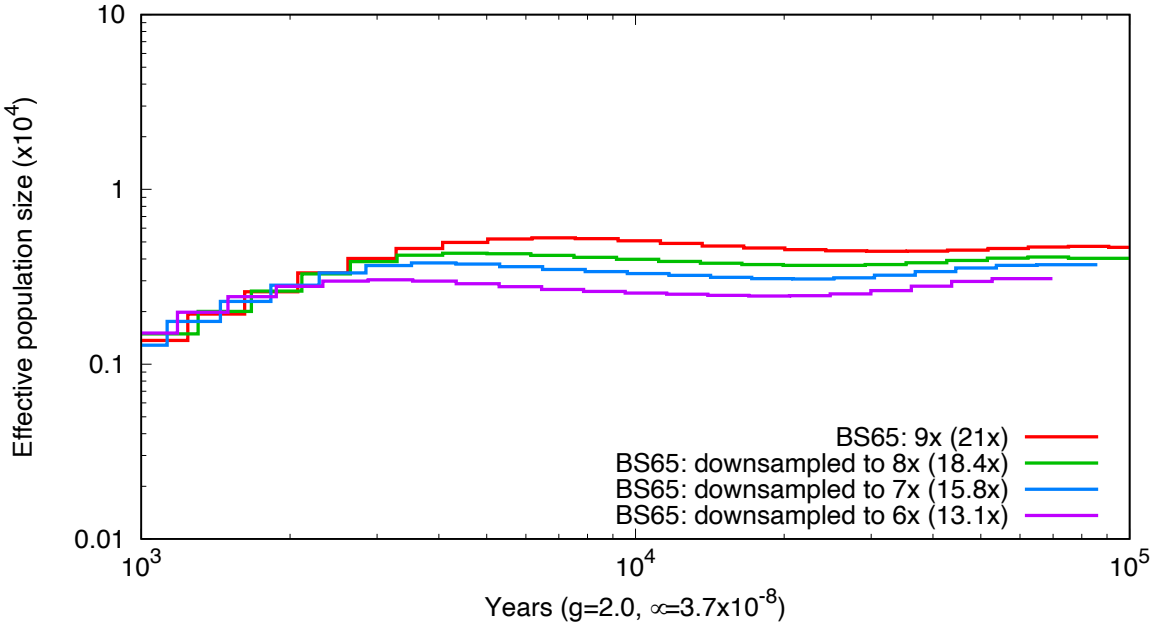

We then estimated PSMC plots of effective population size through time for five highest coverage individuals from each of the three populations to see if plots were consistent across individuals per population. Thick lines represent the genomes included in Figure 3A.

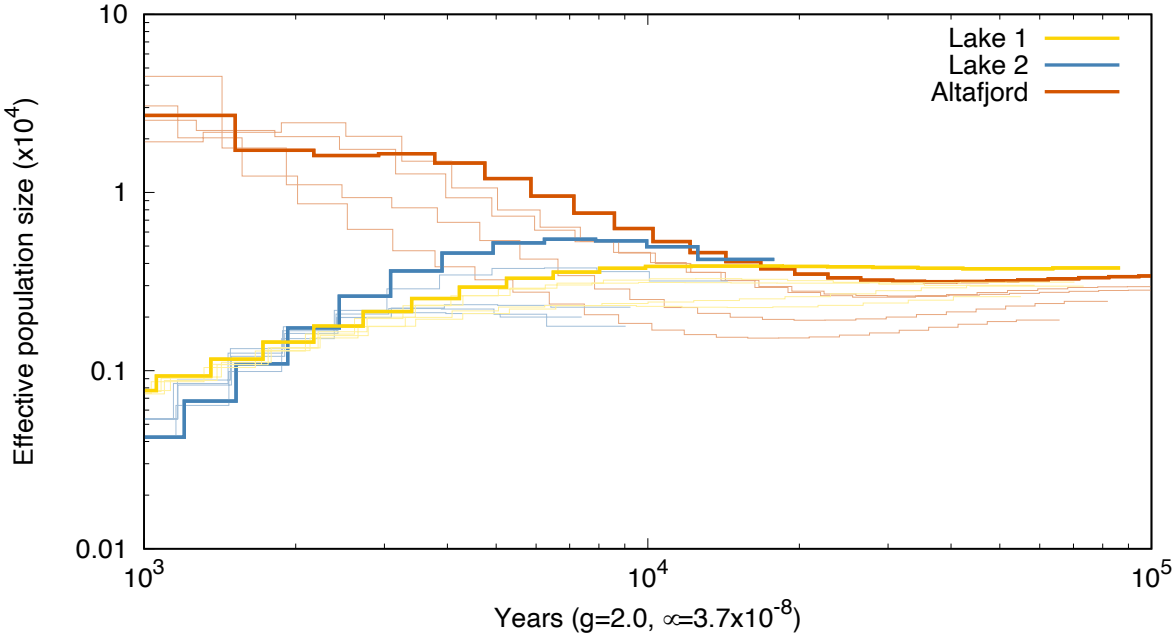

4 Manhattan plots of genome-wide estimates of F_{ST}

Weir and Cockerham's F_{ST} can provide a useful measure of differentiation between populations, but is also sensitive to genetic diversity within populations. We estimated F_{ST} for 10 kb sliding windows at intervals of 5 kb across each chromosome for each. We plotted the results as Manhattan plots and overlaid the positions of runs of homozygosity (ROH) and the location of the 242 divergent regions from Jones *et al.*[S1]. Windows with $F_{ST} > 0.5$ are coloured red and above the dotted marker line. We found outlier peaks in our lake vs fjord comparisons corresponded to many of the regions identified by Jones *et al.*[S1] and to shared ROH >0.3Mb, particularly among individuals from the same lake.

Lake 1 vs Altafjord

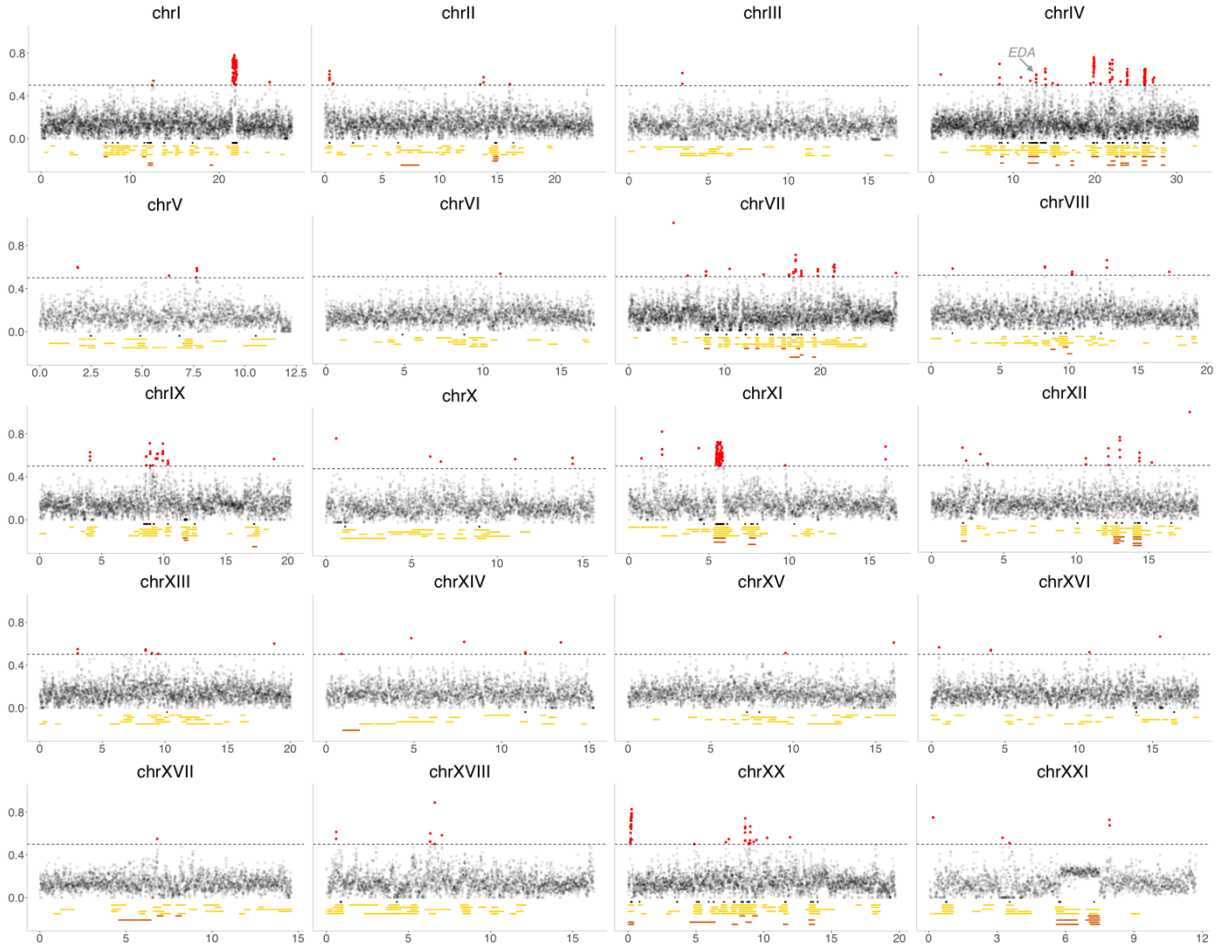

Lake 2 vs Altafjord

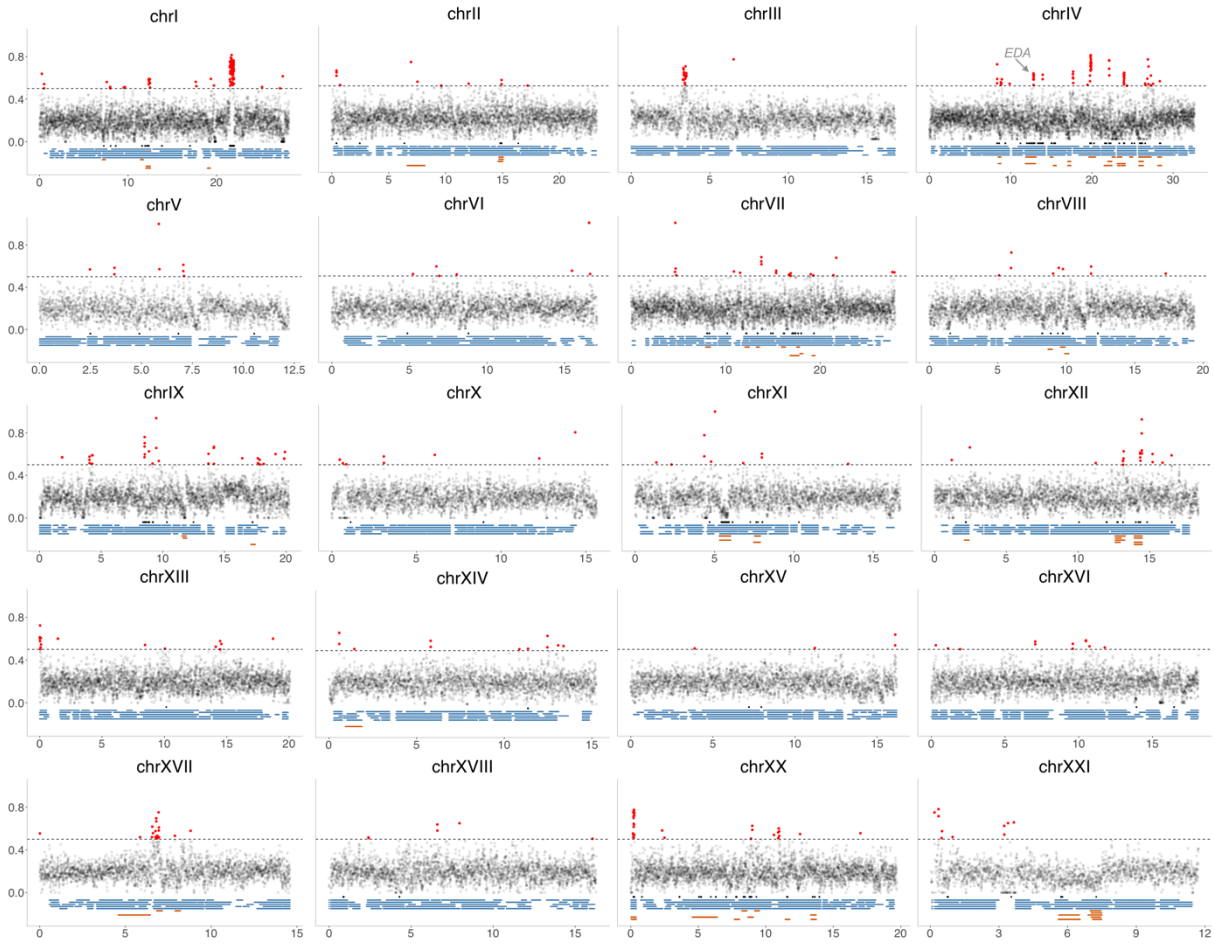

Lake 1 vs Lake 2

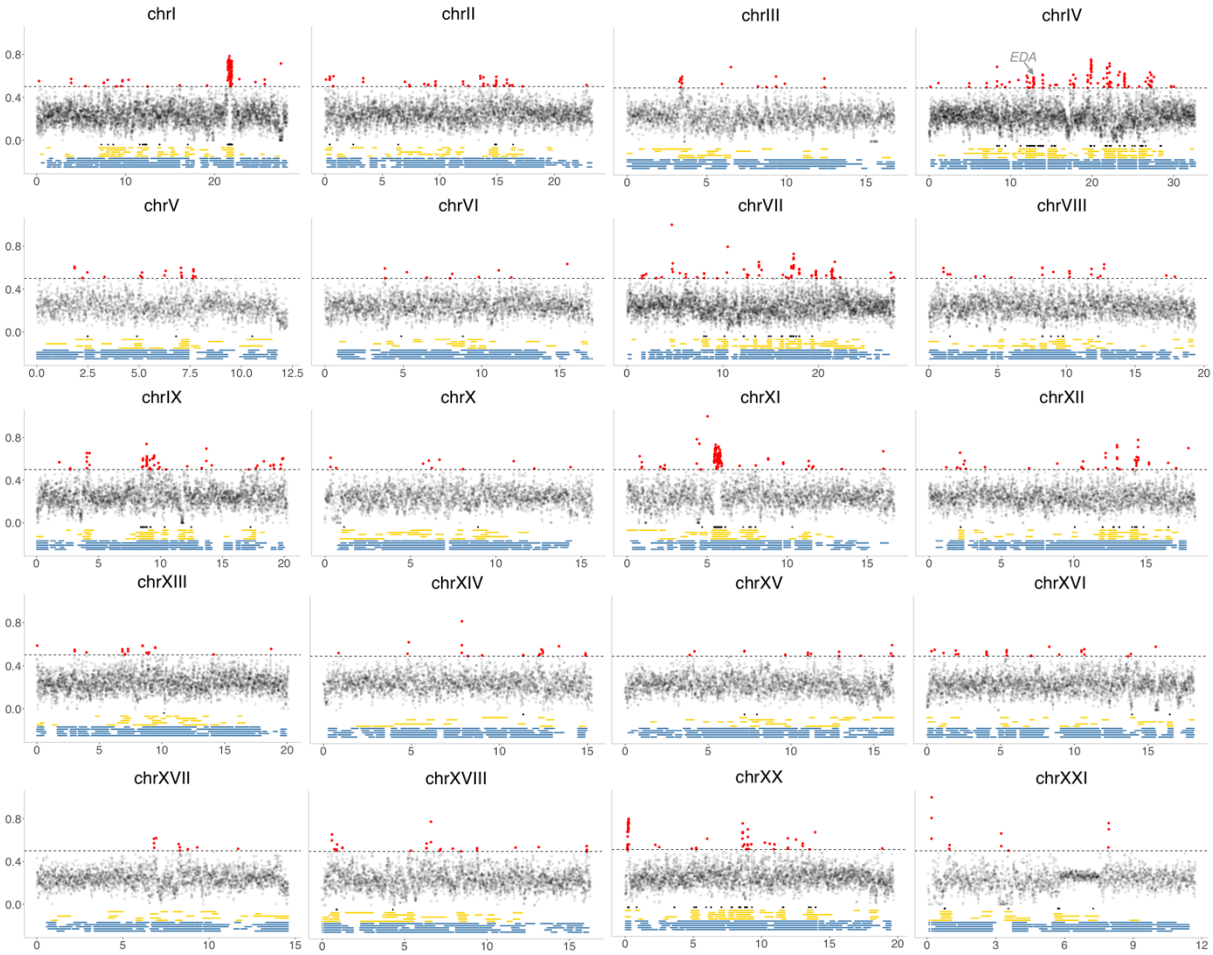

5 Forward simulations were performed using SLiM 3

Forward simulations were performed using SLiM 3[S3] based on the elegant model published in Galloway *et al.*[S4]. During the first 100,000 generations two populations, a continuous marine population and a freshwater population separated into 25 lakes, were used to create an initial standing genetic variation of freshwater-adaptive alleles in the marine population. Each population consists of 5,000 individuals and the migration rate between the two populations is $m = 0.00025$. After 100,000 generations, twenty-five new lakes are colonized by 200 marine individuals each. In contrast to the Galloway model, these lakes were modelled as separate populations and were isolated from the marine population, *i.e.* no migration between the newly introduced lakes and the marine population, or between lakes. The Galloway study simulate a single chromosome of length 1 Gb. In order to study the effects of different recombination rates, we simulate two chromosomes of length 500 Mb with recombination events occurring at a rate of 10^{-8} and 10^{-7} per bp per generation respectively. The mutation rate in this simulation amounts to 10^{-10} per bp per generation. As per the Galloway study, 10 effect regions are spread across the chromosome(s). Within these effect regions, mutations of six different types can arise. Mutations can either be dominant (dom), recessive (rec) or additive (add). Furthermore, each mutation is either beneficial in the marine environment and deleterious in the freshwater environment (mar), or vice versa (fw). The effect sizes for each mutation are chosen randomly from an exponential distribution with a mean ±0.5. Individual trait values are subsequently determined additively from the diploid genotypes and individual fitness is calculated from these individual trait values as in Galloway *et al.*[S4].

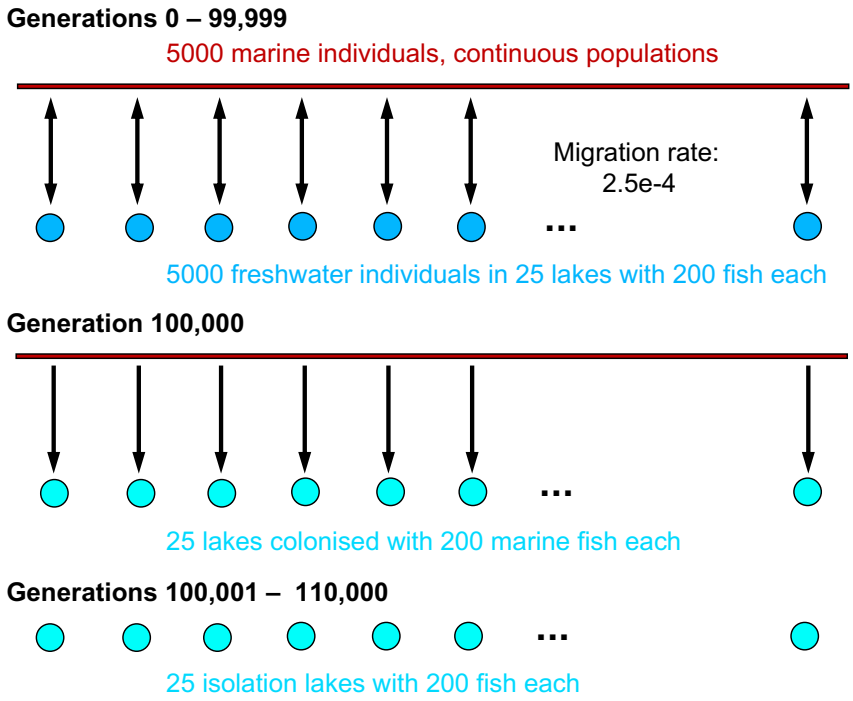

Counts were made of different mutation types in the marine population at generation 100, 1,000, 10,000 and 100,000 – means and standard deviation from 100 simulation runs. Dominant and additive mutations that are beneficial in the marine environment (red) rise to high frequencies over time, mutations that are beneficial in freshwater but deleterious in the marine environment (blue) stay at low frequencies (mostly < 0.1, which corresponds to 10 haplotypes in the whole marine population) and represent standing genetic variation of freshwater-adaptive mutations.

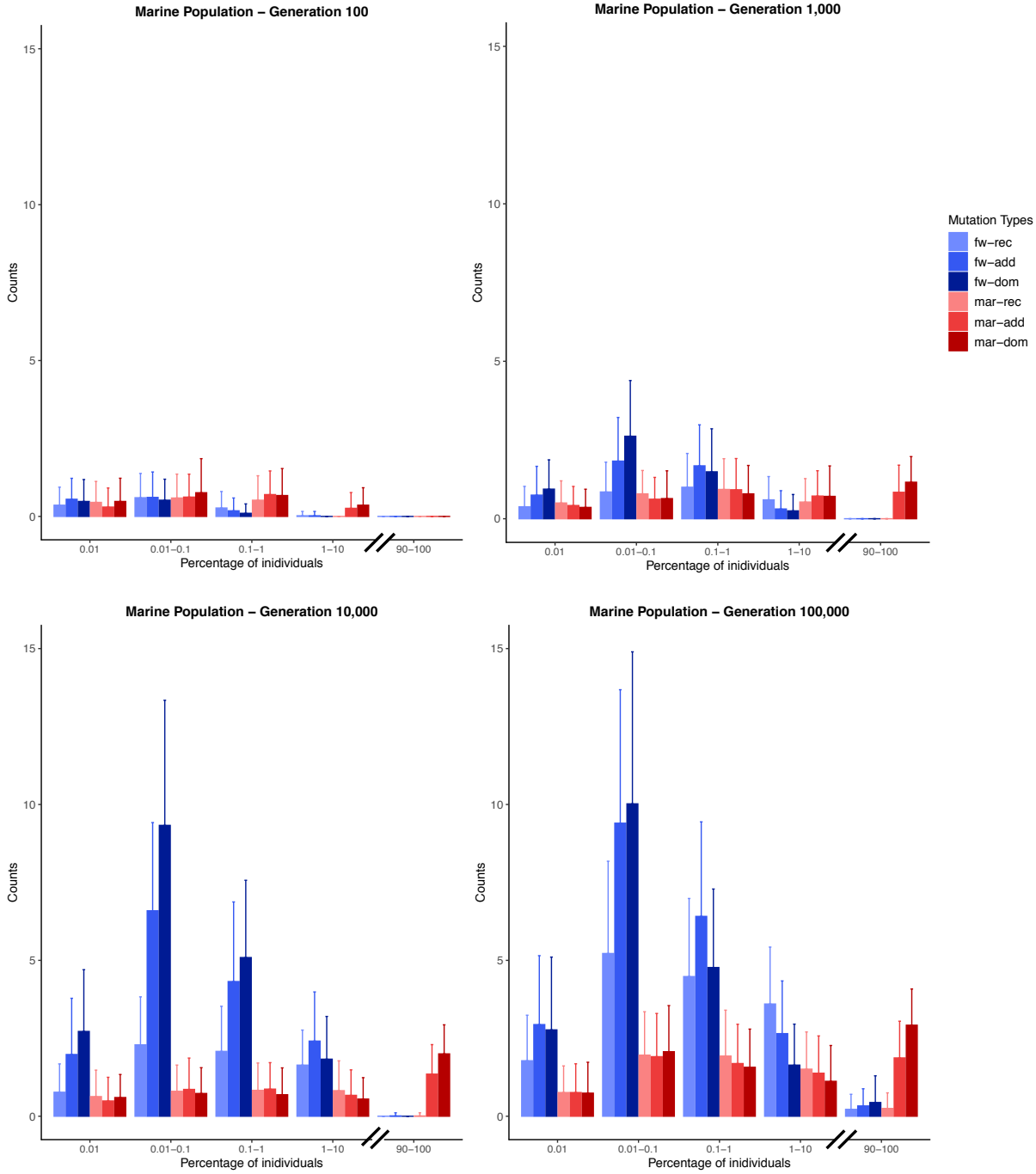

Counts of different mutation types were summed up for all freshwater lakes at generation 100, 1,000, 10,000 and 100,000 – means and standard deviation from 100 simulation runs. Most mutation types occur at a frequency less than 10%, which corresponds to 1,000 haplotypes of all 10,000 haplotypes of freshwater individuals. A mutation at a frequency of 10% in the freshwater population could be fixed in two freshwater lakes.

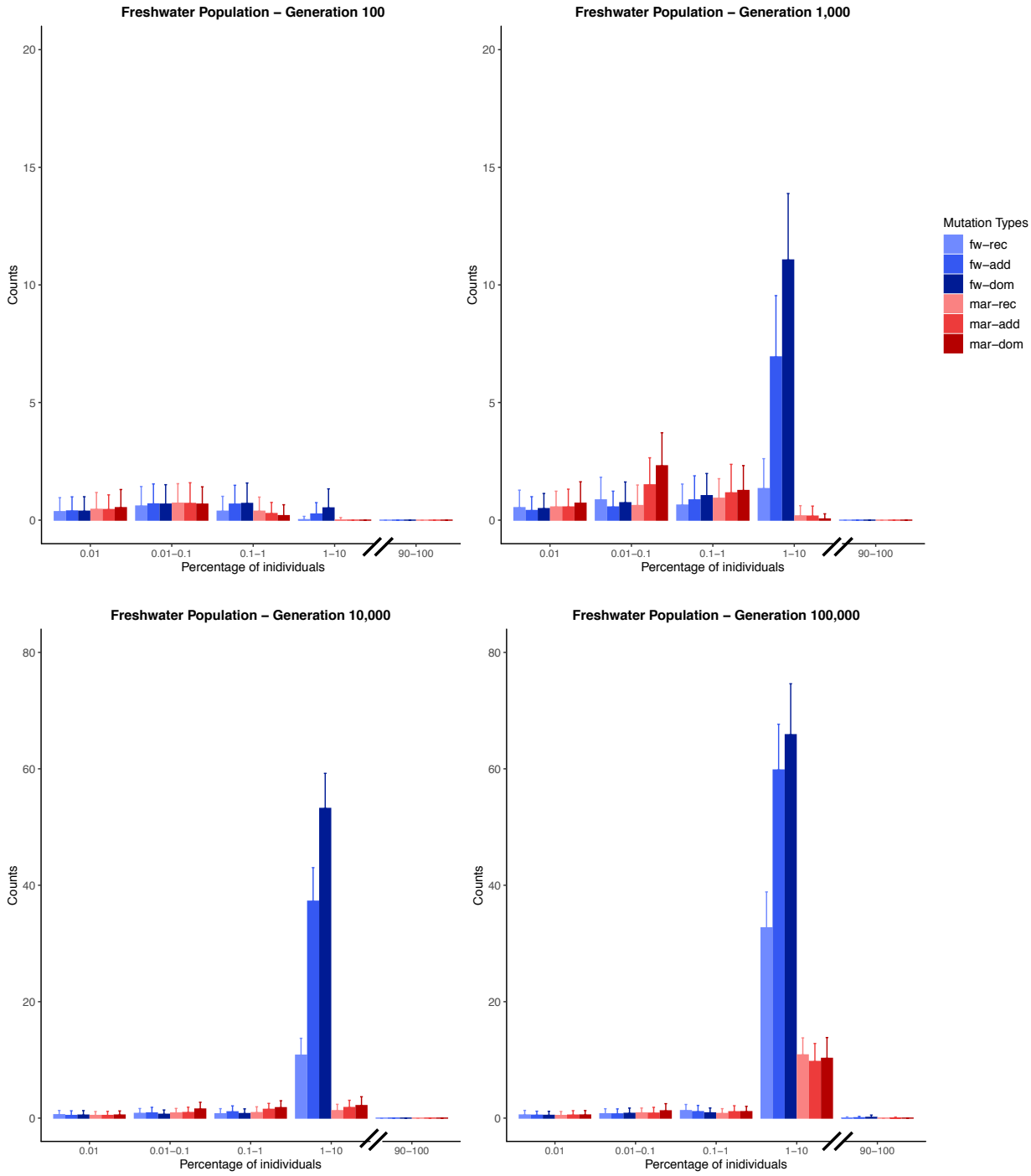

Counts for different mutation types for all isolation lakes at 0, 10, 100, 1,000 and 10,000 generations after colonization from the marine environment – means and standard deviation from 100 simulation runs. Marine-adaptive alleles (red) introduced into the isolation lakes at high frequencies during colonization are retained as fixed substitutions. Freshwater-adaptive mutations (blue) rise to high frequency over time.

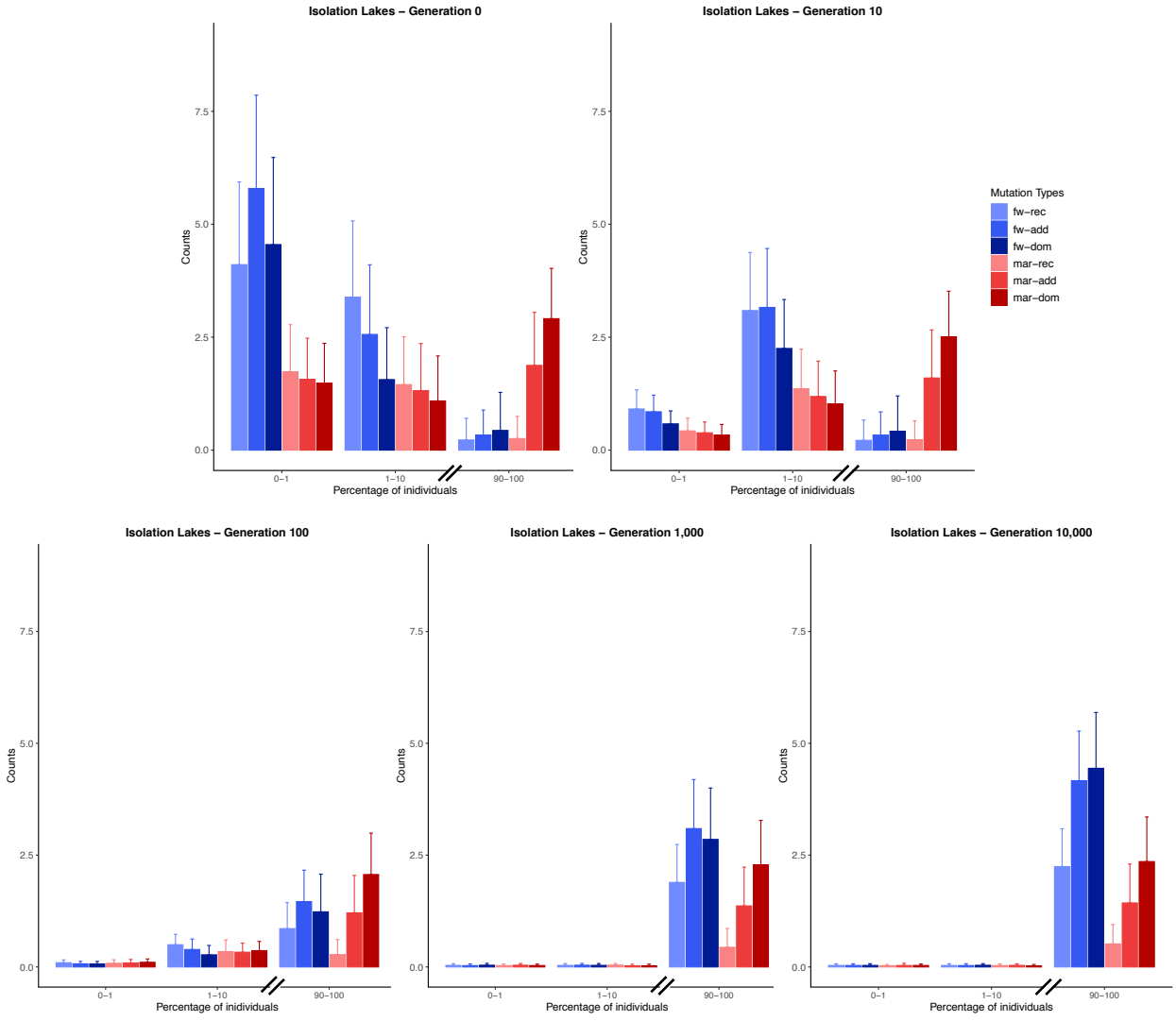

Stacked counts for different mutation types showing the effect of different recombination rates for marine and freshwater populations at generation 100,000 – means and standard deviation from 100 simulation runs. Mutations rising to high frequency appear at similar abundance on the two chromosomes with one chromosome having a recombination rate of 1e-08 (rr-1e-08) and the other 1e-07 (rr-1e-07).

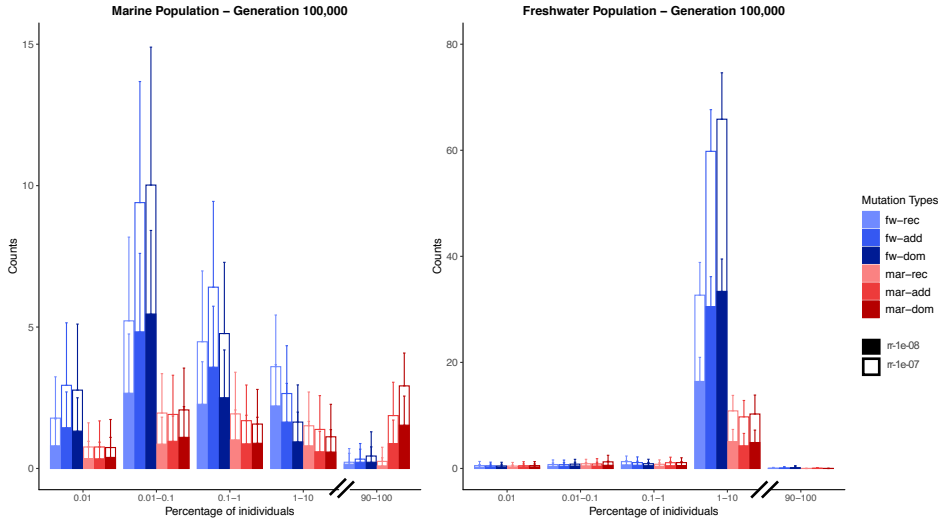

Stacked counts for different mutation types and different recombination rates for all isolation lakes at generation 0, 10, 100, 1,000 and 10,000 after colonization at generation 100,000 – means and standard deviation from 100 simulation runs. Mutations rising to high frequency appear at similar abundance on the two chromosomes with one chromosome having a recombination rate of 1e-08 (rr-1e-08) and the other 1e-07 (rr-1e-07).

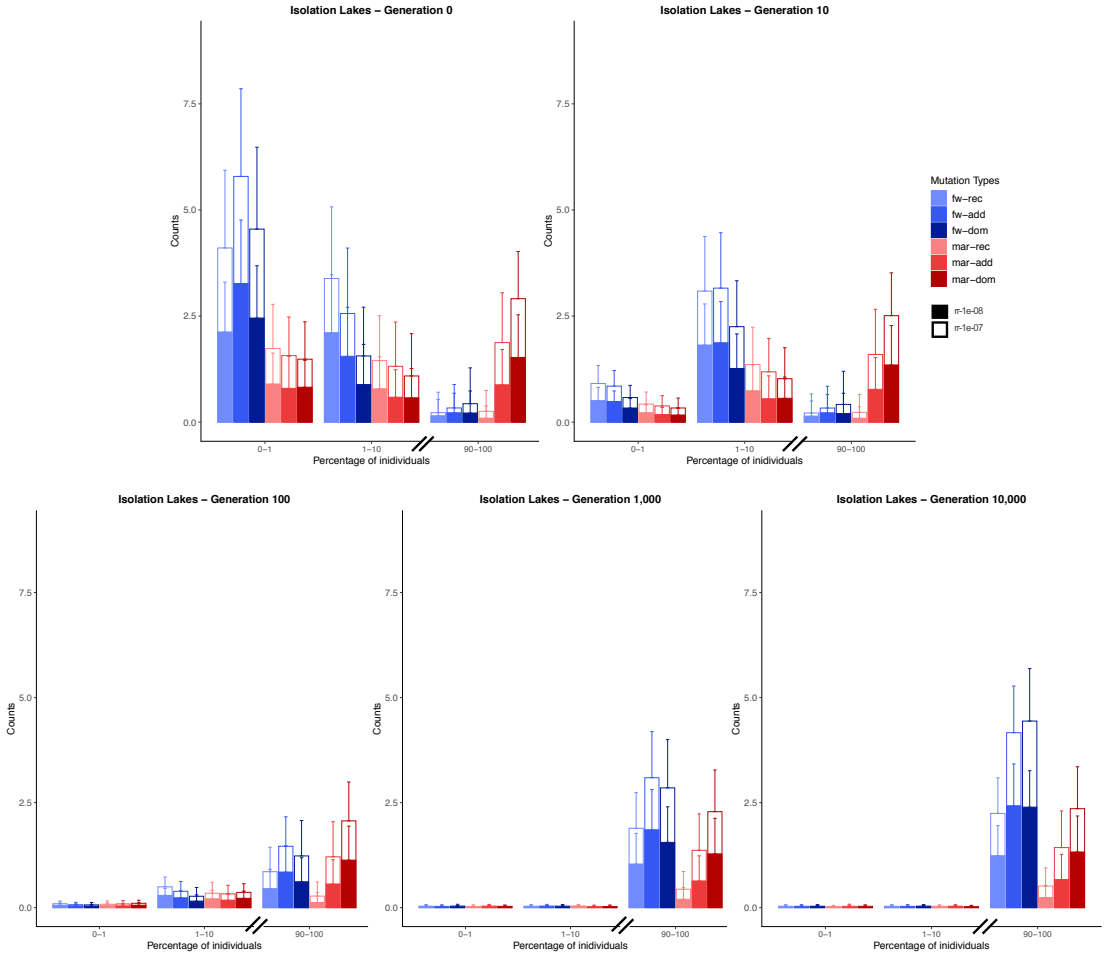

Stacked counts for different mutation types showing the effect of different effect sizes for marine and freshwater populations at generation 100,000 – means and standard deviation from 100 simulation runs. Dominant and additive mutations that are beneficial in the marine environment (red) and at high frequencies (90-100%) in the marine population have mostly a large effect size (> 0.5), whereas these mutation classes with small effect sizes (< 0.5) are more common at low frequencies. Respectively, mutations beneficial in a freshwater environment (blue) at intermediate frequency (here 1-10%) in the freshwater population show large effect sizes (> 0.5), whereas those beneficial in marine environments (red) have mostly low effect sizes (< 0.5).

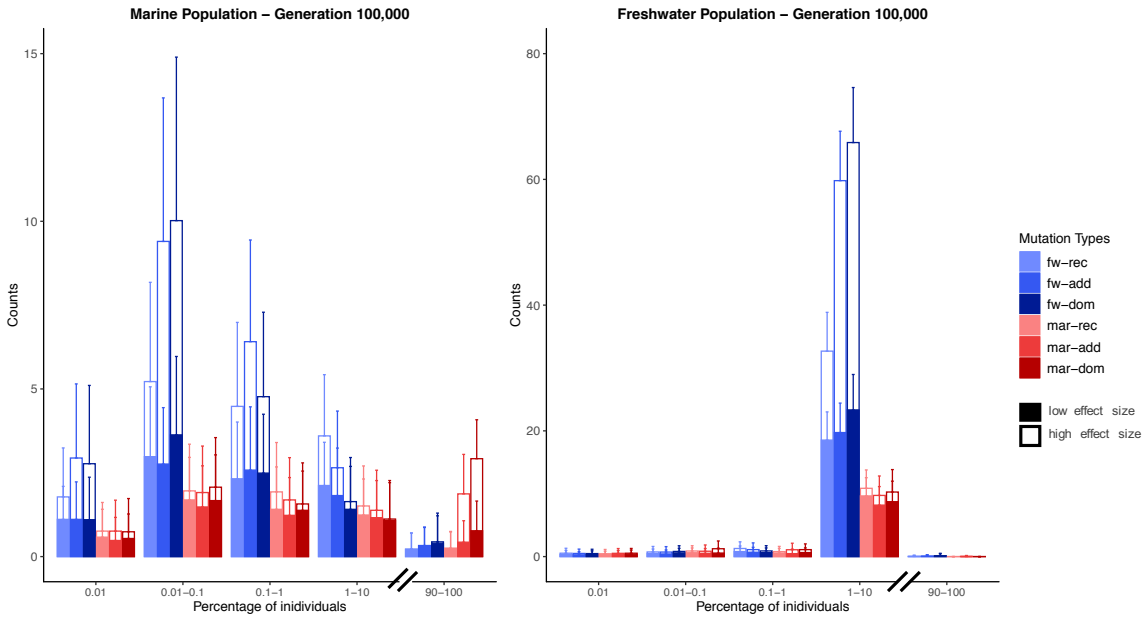

Stacked counts for different mutation types and different effect sizes for all isolation lakes at generation 0, 10, 100, 1,000 and 10,000 after colonization at generation 100,000 – means and standard deviation from 100 simulation runs. Whereas marine mutations (red) decrease in frequency over time, all types of freshwater mutations (blue) rise to high frequency. These mutations show high (> 0.5) and low effect sizes (< 0.5) in a similar abundance.

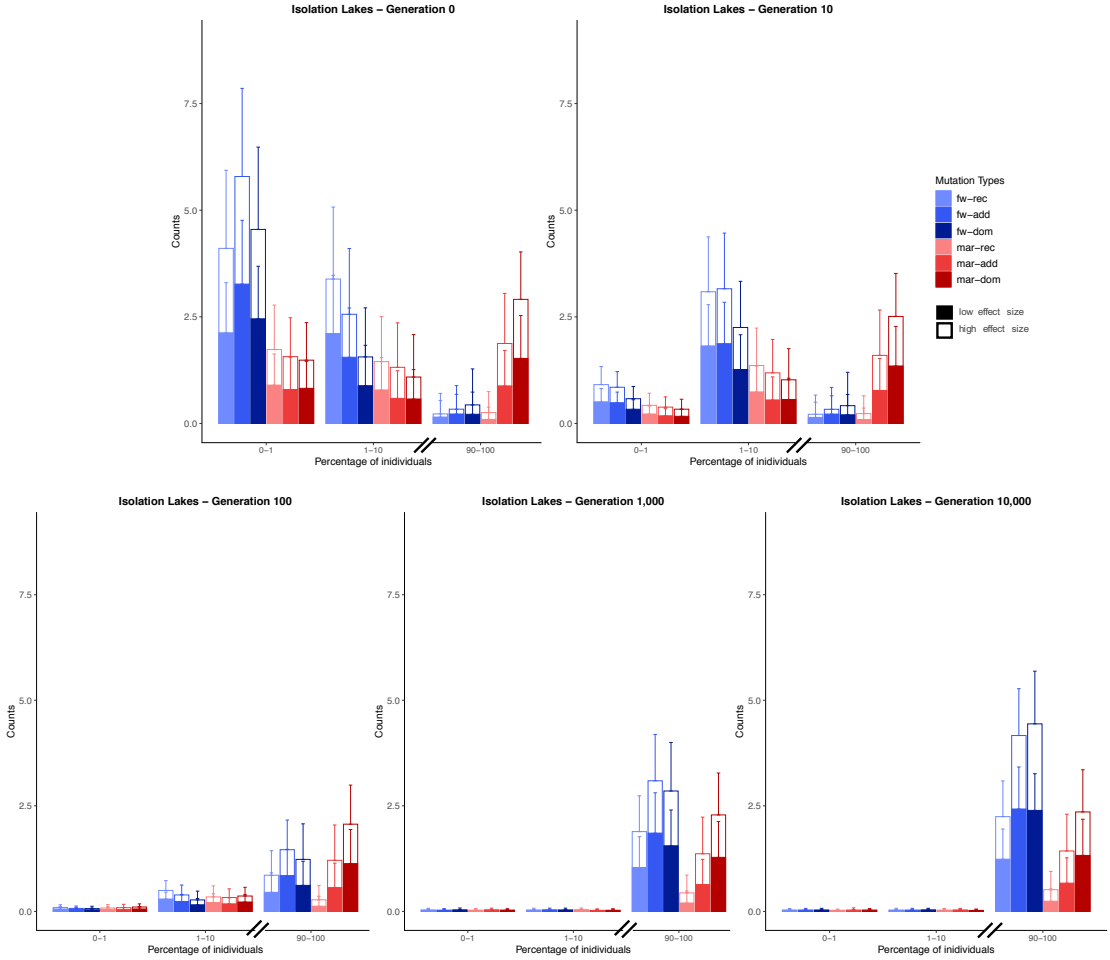

Mean frequency of all mutations from each mutation type in the marine population at generation 100, 1,000, 10,000 and 100,000 for mutations being present in at least one of the isolation lakes until generation 110,000 – means and standard deviation from 100 simulation runs. Marine-dominant as well as freshwater-additive mutations are at high frequencies, whereas freshwater-recessive, freshwater-dominant, marine-recessive and marine-additive mutations are at low frequencies at generation 100,000 in the marine population.

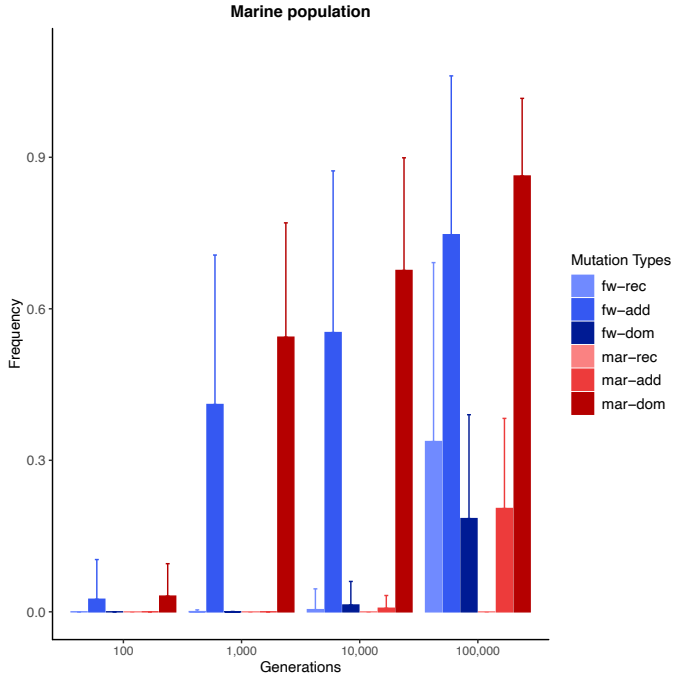

Mean frequency of all mutations from each mutation type in the freshwater population at generation 100, 1,000, 10,000 and 100,000 for mutations being present in at least one of the isolation lakes until generation 110,000 – means and standard deviation from 100 simulation runs. Freshwater as well as marine mutations are present at frequencies between 0 and 0.4 in the freshwater population.

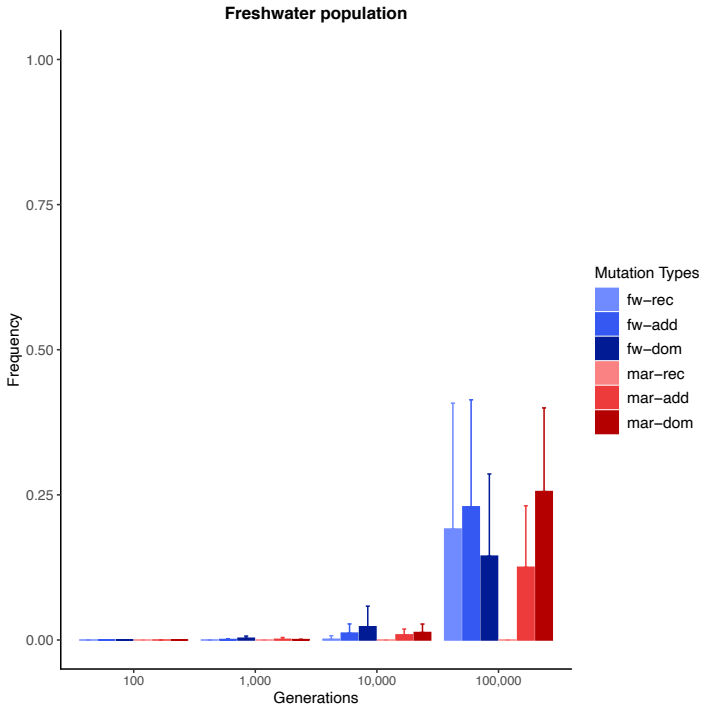

Mean frequency of all mutations from each mutation type in the isolation lakes at generation 0, 10, 100, 1,000 and 10,000 for mutations being present in at least one of the isolation lakes until generation 10,000 after colonization at generation 100,000 – means and standard deviation from 100 simulation runs. Frequencies of mutation types at generation 0 are similar to frequencies in the marine population at generation 100,000. The frequency of all mutation types are increasing over time. Whereas, marine dominant alleles start at high frequency at generation 0, freshwater-dominant and marine-additive mutations rise from low to high frequencies over time.

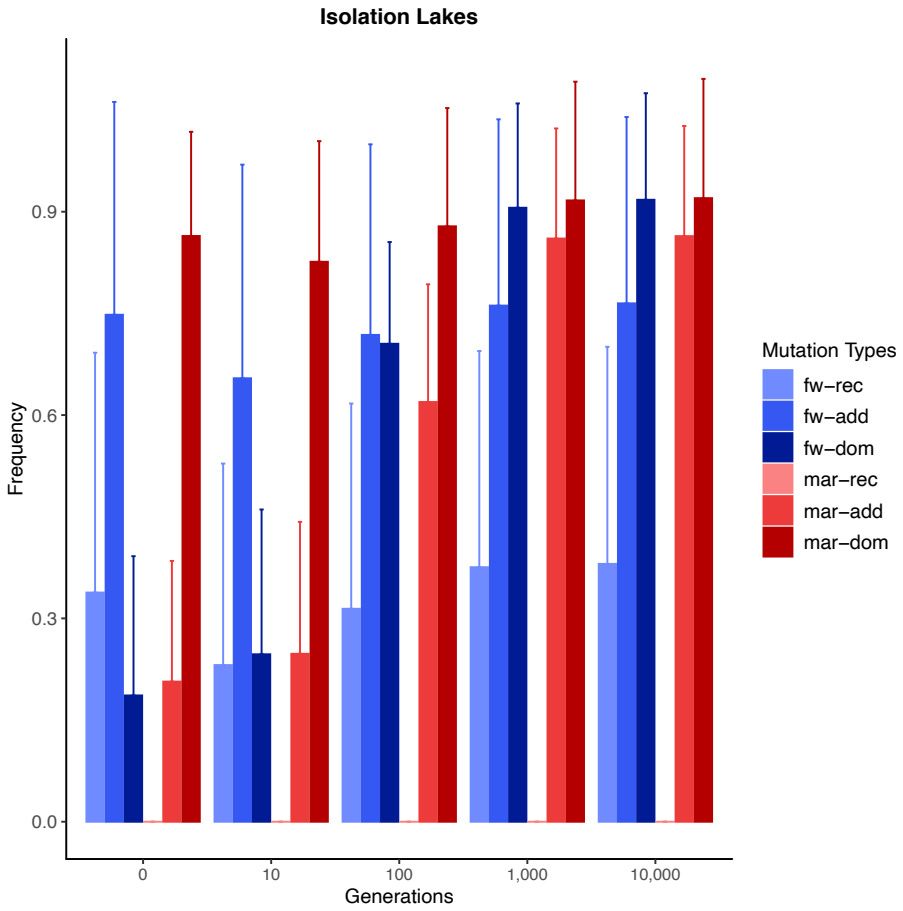

SLiM code is available at https://github.com/Stickle-Back-in-Time/Stickle-Back-in-Time.

6 Sex determination of ancient samples and mitochondrial DNA analysis

Establishing the sex of ancient samples can be important, as haploid markers such as the male X chromosome or Y chromosome, can be used to estimate contamination rates. Sticklebacks have an XY sex-determination system, where males are the heterogametic sex. Males are therefore haploid for the X chromosome and diploid for the autosomes, while females are diploid for both the X chromosome and autosomes. The sex of the ancient samples was determined by comparing the mean coverage of the autosomes (excluding unassembled scaffolds), the pseudoautosomal region (chrXIX:1-3300000 and chrXIX:12270000-20240660), and the sex-determining region (chrXIX:3300000-12270000) among 4 female (red markers) and 4 male (blue markers) modern genomes down-sampled to comparable coverage with each ancient genome.

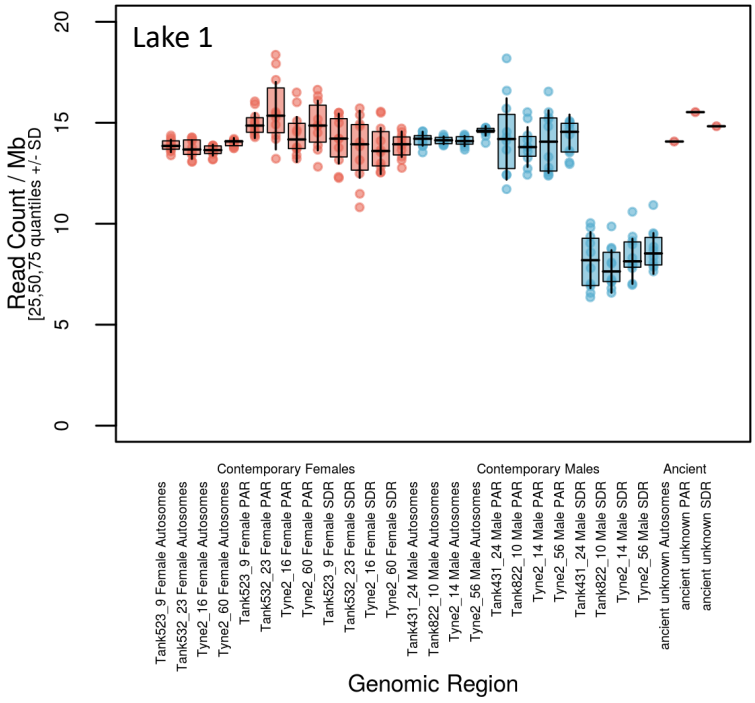

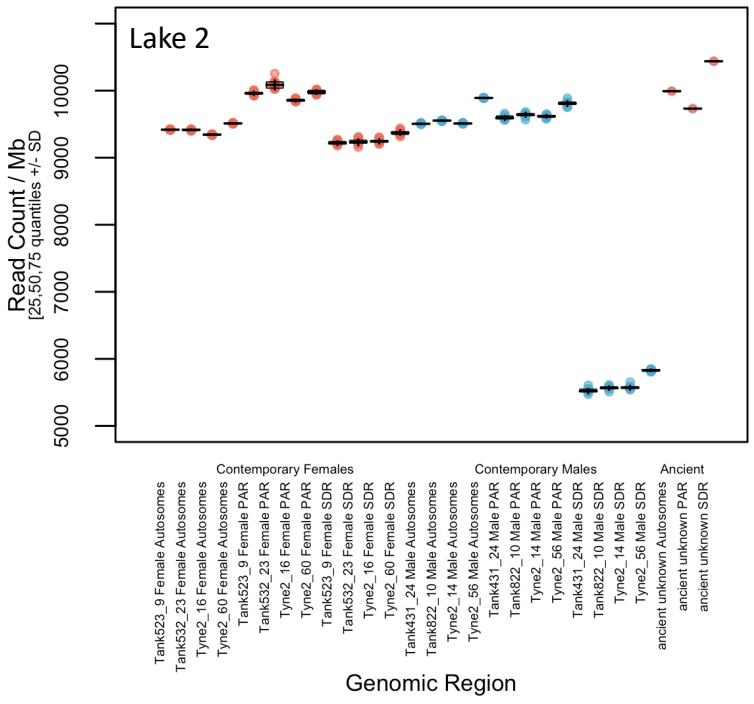

Both ancient samples had approximately equivalent coverage across all three regions implying that both are diploid for the sex-determining region of the X chromosome, *i.e.* are female. For each modern individual the down-sampling was repeated 10 times with different random seeds to initiate the down-sampling. This constrained the analyses of haploid markers to estimate contamination rates in the ancient genomes to the mitochondrial genomes.

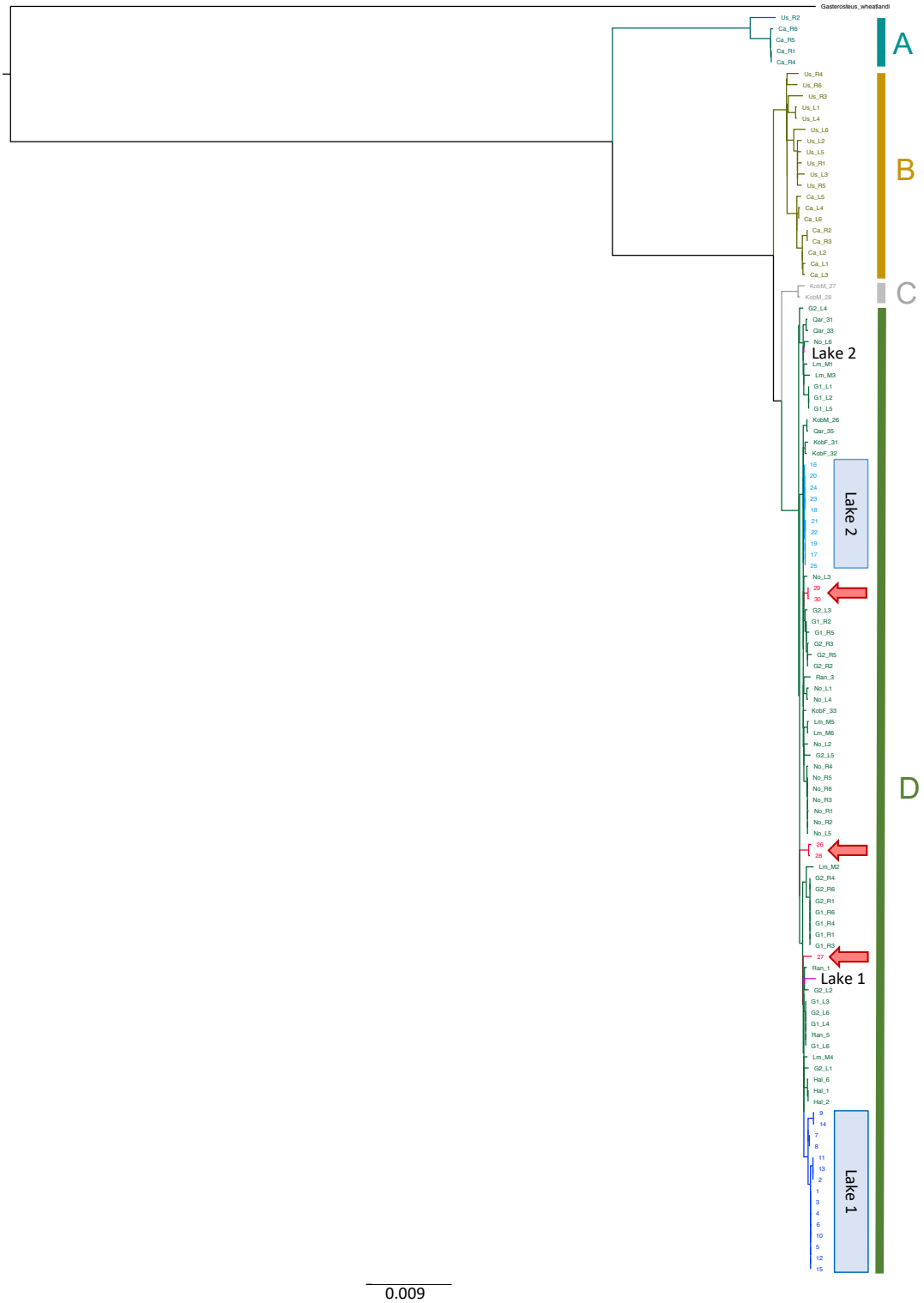

In a maximum likelihood phylogeny of mitochondrial genomes from samples sequenced by this study combined with the dataset used by Liu *et al.*[S5], lineage A corresponds to the

'Japanese Lineage', lineage B to the Pacific part of a major 'Euro-American' lineage, lineage C to the 'Transatlantic Lineage' and lineage D to the 'European Lineage' as per Liu *et al*.[S5]. Modern samples from Lakes 1 and 2 are demarcated by blue boxes, each forms a monophyletic clade with 100% bootstrap support. Samples from Altafjord by red arrows, and the two ancient samples by the black labels 'Lake 1' and 'Lake 2'. Coverage was 1x across most sites, and we detected no heterozygous genotypes in either fish. Furthermore, all segregating sites conformed to the expected haplotype structure based on comparison with modern samples in the same clade. Taken together with the high proportion of reads with DNA damage patterns at the read ends, these results suggest our genome data represented endogenous DNA from the ancient stickleback bones.

Supplemental References

S1. Jones, F.C., Grabherr, M.G., Chan, Y.F., Russell, P., Mauceli, E., Johnson, J., Swofford, R., Pirun, M., Zody, M.C., White, S., *et al.* (2012). The genomic basis of adaptive evolution in threespine sticklebacks. Nature *484*, 55–61.

S2. Feulner, P.G.D., Chain, F.J.J., Panchal, M., Huang, Y., Eizaguirre, C., Kalbe, M., Lenz, T.L., Samonte, I.E., Stoll, M., Bornberg-Bauer, E., *et al.* (2015). Genomics of Divergence along a Continuum of Parapatric Population Differentiation. PLoS Genet *11*, e1004966.

S3. Haller, B.C., and Messer, P.W. (2019). SLiM 3: Forward genetic simulations beyond the Wright–Fisher model. Molecular Biology and Evolution *36*, 632–637.

S4. Galloway, J., Cresko, W.A., and Ralph, P. (2019). A few stickleback suffice for the transport of alleles to new lakes. G3: Genes, Genomes, Genetics *10*, 505–514.

S5. Liu, S., Hansen, M.M., and Jacobsen, M.W. (2016). Region-wide and ecotype-specific differences in demographic histories of threespine stickleback populations, estimated from whole genome sequences. Mol. Ecol. *25*, 5187–5202.

Declaration of Interests form

Click here to access/download

Supplemental Videos and Spreadsheets

DI_form.pdf

Inclusion and Diversity form